

Non-destructive testing and evaluation of composite materials/structures: A state-of-the-art review

Advances in Mechanical Engineering
2020, Vol. 12(4) 1–28
© The Author(s) 2020
DOI: 10.1177/1687814020913761
journals.sagepub.com/home/ade


Bing Wang^{1,2} , Shuncong Zhong², Tung-Lik Lee³,
Kevin S Fancey⁴ and Jiawei Mi⁴

Abstract

Composite materials/structures are advancing in product efficiency, cost-effectiveness and the development of superior specific properties. There are increasing demands in their applications to load-carrying structures in aerospace, wind turbines, transportation, medical equipment and so on. Thus, robust and reliable non-destructive testing of composites is essential to reduce safety concerns and maintenance costs. There have been various non-destructive testing methods built upon different principles for quality assurance during the whole lifecycle of a composite product. This article reviews the most established non-destructive testing techniques for detection and evaluation of defects/damage evolution in composites. These include acoustic emission, ultrasonic testing, infrared thermography, terahertz testing, shearography, digital image correlation, as well as X-ray and neutron imaging. For each non-destructive testing technique, we cover a brief historical background, principles, standard practices, equipment and facilities used for composite research. We also compare and discuss their benefits and limitations and further summarise their capabilities and applications to composite structures. Each non-destructive testing technique has its own potential and rarely achieves a full-scale diagnosis of structural integrity. Future development of non-destructive testing techniques for composites will be directed towards intelligent and automated inspection systems with high accuracy and efficient data processing capabilities.

Keywords

Non-destructive testing, composite materials, structures, defects, damage, detection and evaluation, structural health monitoring

Date received: 11 November 2019; accepted: 25 February 2020

Handling Editor: James Baldwin

Introduction

Composite materials/structures are advancing in product efficiency, cost-effectiveness and the development of superior specific properties (strength and modulus). There are increasing demands in their applications to load-bearing structures in aerospace, wind turbines, transportation, medical equipment and so on.¹ Manufacturing of composite materials is a multivariable task, involving many procedures, where various types of defects may occur within a composite product, giving rise to significant safety concerns in service.²

¹Department of Engineering, University of Cambridge, Cambridge, UK

²School of Mechanical Engineering and Automation, Fuzhou University, Fuzhou, China

³ISIS Neutron and Muon Source, Rutherford Appleton Laboratory, Didcot, UK

⁴Department of Engineering, University of Hull, Hull, UK

Corresponding author:

Bing Wang, Department of Engineering, University of Cambridge, Cambridge CB2 1PZ, UK.
Email: bw407@cam.ac.uk



Detection and evaluation to maintain structural integrity are particularly challenging since composites are usually non-homogeneous and anisotropic. Defects and damage can occur within numerous locations at various levels of scale, making it difficult to track all the damage sites which can result in complex damage mechanisms.³ In addition, damage accumulation within a composite is closely related to the actual strength, stiffness and lifetime prediction of the component. Therefore, robust and reliable non-destructive testing (NDT) of composites is essential for reducing safety concerns, as well as maintenance costs⁴ to minimise possibilities for process disruption and downtime. These factors attract interest from both academic researchers and industrial engineers.

There are a wide variety of NDT techniques built upon different principles. These have demonstrated effectiveness in quality assurance throughout the whole lifecycle of composite products, that is, in process design and optimisation, process control, manufacture inspection, in-service detection and structural health monitoring.⁵ There are reviews available on NDT methods used for composite research over different timelines, focusing on various aspects: for general methods and trends over last 30 years refer to,^{4,6–11} specific areas include those which concentrate on porosity in composite repairs,¹² crack damage detection,¹³ bond defect determination in laminates,¹⁴ thick-wall composites,¹⁵ sandwich structures,^{16,17} large-scale composites,¹⁸ smart structures,¹⁹ as well as inspection and structural health monitoring of composites,^{20,21} especially for marine,²² wind turbine^{23–26} and aerospace applications.^{27,28} Audiences are recommended to refer to further information on their specific interests.

This article reviews the most established NDT techniques for detection and evaluation to ensure the structural integrity of composite materials/structures; however, a full description of all methods is beyond the scope of this article. Instead, we aim to provide a practical review of the established and emerging NDT techniques and their applications to composite research. The American Society for Testing and Materials (ASTM) has developed more than 130 standards, guides and practices, containing technical specifications, criteria, requirements, procedures and practices for most of the NDT techniques.²⁹ We also include the standard practices for each NDT method available from the ASTM to provide guidance for researchers and engineers. These make it a unique state-of-the-art review article to cover the most up-to-date practical information for NDT techniques and their applications to composite materials and associated structures.

The article is organised as follows. Section ‘Defects and damage evolution in composites’ introduces the potential defects and damage evolution in composites. Section ‘NDT and evaluation techniques’ provides an

overview of development and principles of NDT techniques and then elaborates on eight well-established NDT methods in subsections, covering a brief historic background, principles, standard practices, equipment and facilities for each NDT method in composite research. These include visual inspection (VI), acoustic emission (AE), ultrasonic testing (UT), infrared thermography (IRT), terahertz (THz) testing, shearography, digital image correlation (DIC), as well as X-ray and neutron imaging (NI) and these are described in sections ‘VI’, ‘AE’, ‘UT’, ‘IRT’, ‘THz’, ‘Shearography’, ‘DIC’, ‘XRI’ and ‘NI’, respectively. Section ‘Conclusion and outlook’ compares and discusses the benefits and limitations of above NDT techniques and further summarises their capabilities and applications to composite structures. This article is concluded by the further development of NDT techniques, which is driven by intelligent and automated inspection systems with high accuracy and efficiency in data processing.

Defects and damage evolution in composites

Manufacturing-induced flaws/defects can occur in many forms: unevenly distributed fibres cause resin-rich regions; laminate–tool interactions result in in-plane fibre waviness or out-of-plane fibre wrinkling,^{30,31} voids and porosities arise from poor resin infusion; inclusions from contaminated ambient conditions; misalignment of ply and fibre orientation; matrix cracking, laminate warping and buckling from build-up of thermal residual stresses during curing and so on.^{32,33} Flaws/defects act as stress concentration points, promoting crack propagation and delamination to reduce effective strength, stiffness and service time of composite products.³⁴ Although residual stresses can occasionally be beneficial, especially for producing morphing composite structures,^{35–38} they are usually detrimental.³² A wide range of processes have been developed for the moulding of composite materials to reduce flaws, defects and build-up residual stresses that may occur during manufacture. These can involve multi-step processing, expensive consumables and equipment, to meet technical requirements. Typical industrial practice generally includes NDT inspection and evaluation of composite products to ensure their structural integrity and mechanical performance, which can be particularly challenging.³⁹

Figure 1 summarises the typical flaws and defects that may occur during manufacturing and the in-service damage evolution of a composite material/structure. There are no clear boundaries on the scales of different defects and damage (which also depend on composite constituents); thus, here we provide general guidance according to the published literature.

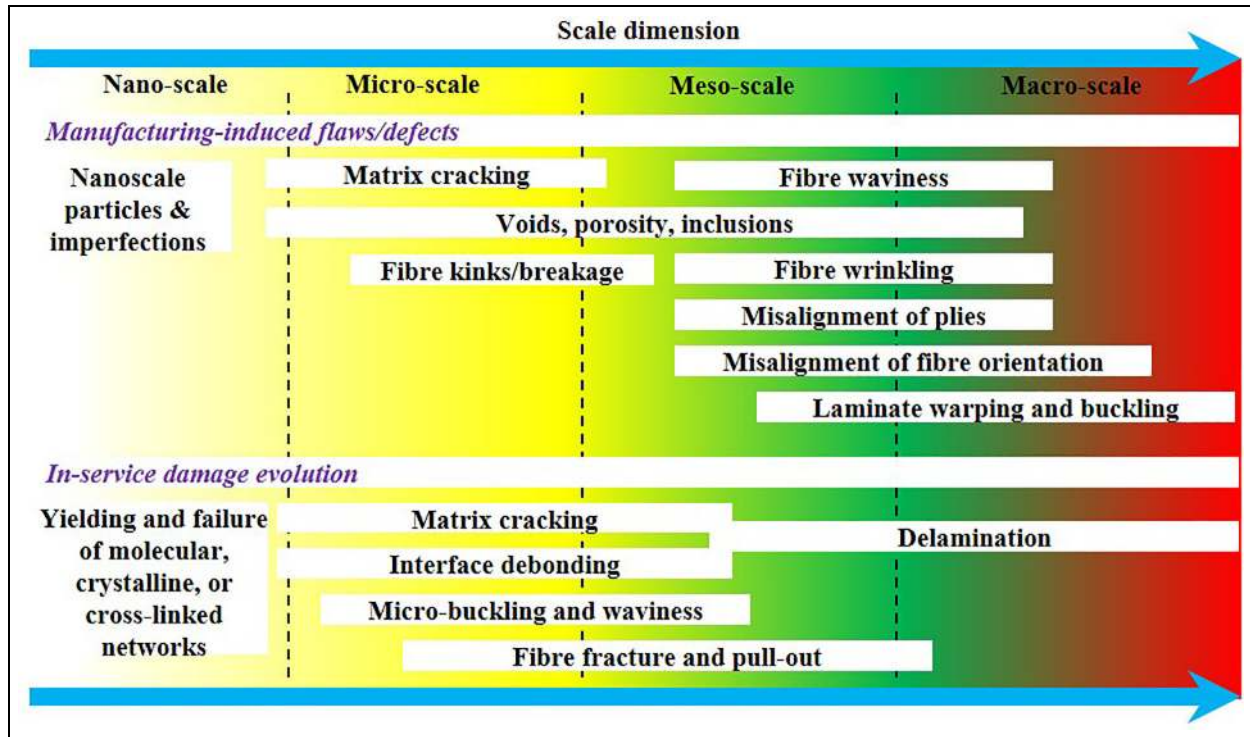


Figure 1. Manufacturing-induced flaws/defects, and in-service damage evolution of a composite material/structure, with their potential scale dimensions.

In-service damage evolution within a composite material/structure depends on composite constituents and loading conditions. Their failure processes are an accumulation of basic rupture mechanisms that include matrix cracking, fibre/matrix debonding, fibre fracture and pull-out, micro-buckling and waviness, delamination and so on.^{40,41} The damage process initiates at the nano- or micro-scale, where molecular chains, crystals and amorphous regions (for semi-crystalline thermoplastic polymers) or cross-linked molecular networks (for thermosetting polymers) carry loads until their limits are reached; damage then starts to accumulate on the micro-scale through crack propagation, interface debonding and micro-buckling, fibre fracture and pull-out, which lead to delamination, ultimately developing into macro-scale failure of the composite.

NDT and evaluation techniques

The term ‘NDT’ covers a wide range of analytical techniques to inspect, test or evaluate chemical/physical properties of a material, component or system without causing damage. Early established NDT techniques include ultrasonic, X-ray radiography, liquid penetrant testing (LPT), magnetic particle testing and eddy-current testing, which were initially developed for steel industry. Among these, ultrasonic and radiographic detection are also effective inspection techniques for

composite structures.¹⁷ It is difficult to select appropriate NDT techniques for a specific purpose; however, ASTM E2533⁵ serves as a practical guide in using NDT methods on composite materials/structures for aerospace applications.

To date, there have been numerous NDT methods based on different principles, see Figure 2. They can be categorised into five groups: (1) VI (i.e. those visible to the human eye); (2) acoustic wave-based techniques, such as AE, nonlinear acoustics and ultrasonic waves; (3) optical techniques, which include IRT, THz testing, shearography, DIC; (4) imaging-based techniques, for example, X-ray/neutron radiography/tomography and micro-tomography;⁴ (5) electromagnetic field-based techniques, such as eddy-current testing, remote field testing, magnetic particle inspection and magnetic flux leakage testing.⁴²

Here, we focus on eight established and emerging NDT techniques and their applications to composite research in categories (1) to (4), with the exclusion of category (5). Since NDT methods in category (5) are based on electromagnetic induction, their applications are limited to conductive materials.⁴³ Eddy-current testing (ECT), for example, is well established and widely used for detecting cracks and corrosion in homogeneous metallic materials. Although it may be applicable to carbon composites, their conductivities are usually very low and inhomogeneous due to the layup and

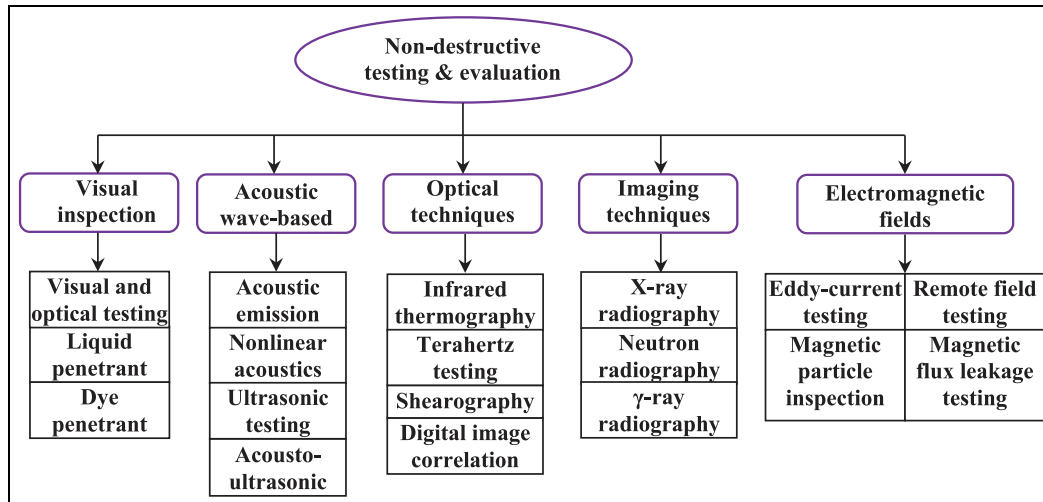


Figure 2. Categories of non-destructive testing and evaluation techniques.

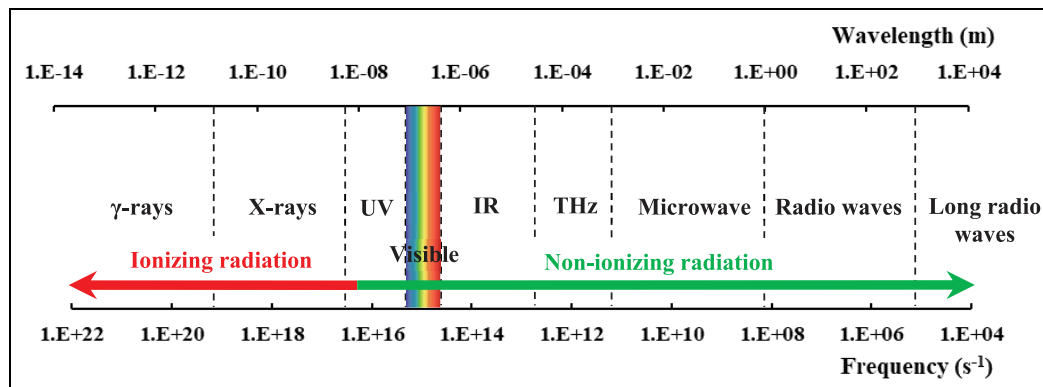


Figure 3. Diagram of the electromagnetic spectrum, defining the various regions of radiation according to their range of frequencies and wavelengths.

bundling of the conductive fibres.⁴⁴ This leads to further issues and difficulties for ECT to be an efficient and cost-effective solution for most composite NDT applications.

The measurement principles of each elaborated NDT technique depend on the characteristics of the electromagnetic waves based. Figure 3 shows the electromagnetic spectrum with divided wavelength sub-regions: the soft boundaries indicate terminologies for the subsections. Developments in generation and detection within each spectral regime have induced numerous industrial applications.⁴⁵ Ionising radiation consists of short-wave ultraviolet (UV), X-rays, gamma-rays or highly energetic particles, such as α -particles, β -particles or neutrons, which are harmful to biological tissues, whereas the remaining part of the spectrum is considered to be non-ionising radiation.

To date, there have been a growing number of research activities in this field. We performed an

electronic database search on articles published in last 30 years (until 31 December 2019) using the Web of Science Core Collection database, to trace the trends in using various NDT techniques within composite research, see Figure 4. The use of AE on composites has a long history and is well established; it is still active in a relatively steady state. Due to significant developments in equipment manufacture, computing power, imaging processing and acquisition techniques over last three decades, there have been rapid increases in the application of IRT, ultrasonic, DIC and X-ray imaging (XRI) to non-destructive detection and evaluation of composite materials/structures. THz-based NDT technology has become a promising technique for composite inspection within the last decade.^{46,47} Research articles on the shearography technique are less, but it was promoted significantly by the invention of the laser in the 1960s;⁴⁸ thus, it is well-established and widely used for industrial NDT, especially in aerospace.^{49,50}

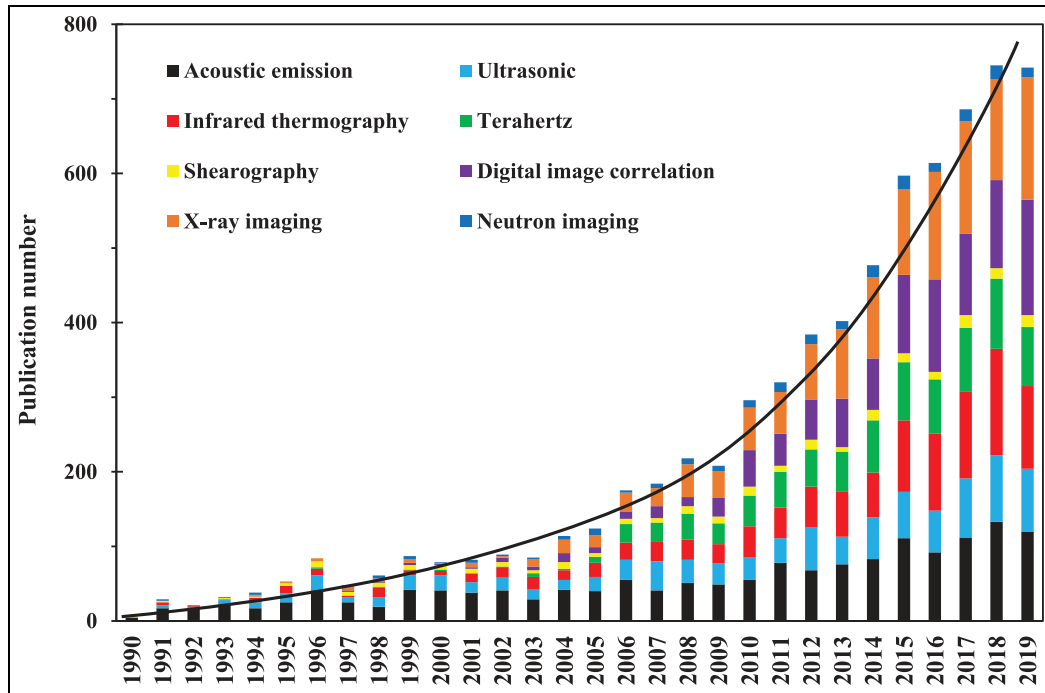


Figure 4. A comparison of publication numbers on various NDT methods and their applications to composite materials/structures in the last 30 years; data are retrieved from Web of Science Core Collection database.

Although NI shares similar principles to XRI, the generation of neutrons is more expensive than for X-rays, the former requiring either a nuclear reactor or spallation process.⁵¹ This has resulted in relatively few publications on its application to composite materials.

VI

VI is the most basic type of NDT technique to inspect damage. It is quick, economically viable and flexible, while its disadvantages are quite obvious and significant.¹¹ VI methods include visual and optical testing (VOT) and LPT. VOT analysis is a leading procedure in the monitoring of surface imperfections for acceptance–rejection criteria during composite parts production.⁵² The LPT technique is a widely applied, low-cost inspection method. It has been used in non-porous materials to detect casting, forging and welding surface defects including cracks, surface porosity, leaks in new products, in-service fatigue cracks and so on.

VI methods are particularly effective in detecting macroscopic flaws, such as poor joints, erroneous dimensions, poor surface finish and poor fits. It usually employs easy-to-handle equipment such as miniature cameras or endoscopes.²³ VI studies of small integrated circuits have shown that the modal duration of eye fixation from trained inspectors was ~ 200 ms. Here, variation by a factor of six in inspection speed led to a variation of less than a factor of 2 in inspection

accuracy; inspection accuracy also depends on training, inspection procedures and apparatus (optics, lighting, etc.).⁵³

AE

Damage occurrences within a composite produce localised transient changes in stored elastic energy; the energy releases stress waves, resulting in fibre breakage, matrix cracking, debonding, delamination and so on.³ AE-based NDT techniques detect and track these sudden releases of stress waves through arrays of highly sensitive sensors or transducers,⁵⁴ as illustrated in Figure 5. Use of the AE method started in the early 1950s when Kaiser⁵⁵ first used electronic instrumentation to detect audible sounds produced by tensile deformation of a metallic specimen. His discovery on the effect of sample stress history on the production of AE became known as the ‘Kaiser effect’.⁵⁶ AE was first applied to the study of composite materials in the 1970s,³ and it has now been widely used in various aspects of composite research.⁵⁷

The AE method is unique in that (1) the signals, i.e. stress waves, are emitted by the testing sample, not from external sources (as with other NDT methods); (2) strain or displacement data are usually recorded, rather than as geometrical defects; (3) it monitors dynamic processes in a material, tracking the development of certain defects, which significantly benefits

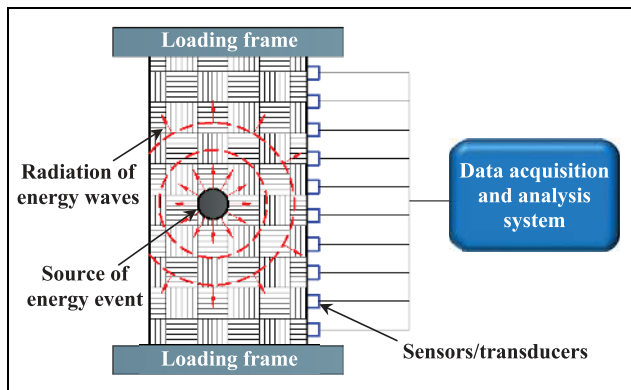


Figure 5. Schematic of localised transient changes in stored elastic energy within a material system under loading, showing the measuring principle of the acoustic emission-based NDT technique.

fatigue tests. It has been reported that AE-based NDT can detect fatigue cracks, fibre fractures, matrix micro-cracks, interface debonding as well as delamination.¹¹ However, there are also certain difficulties. Data collected during the loading of a composite system can be in different forms; the most common is the AE amplitude signal. Processing and analysis of data are time-consuming and require certain skills and experience:³ in particular, the distribution of amplitudes exhibits overlapped areas, which sometimes causes difficulties in associating these with the damage mechanisms.

Efforts have been made to address these issues. A common approach is to analyse multiple parameters to complement the damage analysis, such as cumulated event counts,^{58,59} energy,⁶⁰ duration⁶¹ or frequency of the received amplitude signals.⁶² Other solutions include verifying damage modes through other methods, for example, microscopy, to provide more reliable analysis.⁶³ Standardised practices of using AE include ASTM E1067⁶⁴ on examining glass fibre-reinforced plastic (GFRP) tanks/vessels; ASTM E1118⁶⁵ on composite pipes; ASTM E2191⁶⁶ on filament-wound

composite pressure vessels; ASTM E2076⁶⁷ on composite fan blades as well as ASTM E2661⁶⁸ on plate-like and flat composite structures for aerospace. Table 1 summarises some of the commercial suppliers of AE-based NDT systems, which may be applied to composite research.

There is also some interest in a combined method of AE and UT, namely the acousto-ultrasonic technique (AUT), as first introduced by Vary⁷⁵ in 1981. By adopting the ultrasonic transducer, repeated ultrasonic pulses are introduced into a material, and resultant waveforms carry the morphological information that contributes to damage mechanisms. A concept of 'stress wave factor' is defined as a relative measurement of efficiency of energy dissipation to indicate regions of damage.⁷⁶ In NDT, the AUT is mainly used to determine the severity of internal imperfections and inhomogeneities in composite materials.¹¹

UT

UT is an acoustic inspection technique, which is expanding rapidly into many areas of manufacturing and in-service detection.⁷⁷ It operates through surface wave testing, bulk wave propagation and guided wave propagation, while the guided wave analysis technique is superior for anisotropic materials.⁷⁸ For further information, the use of ultrasonic bulk wave testing in the sizing of flaws has been reviewed by Felice and Fan.⁷⁹ For NDT inspection of composite materials, elastic waves or 'Lamb waves' propagate in selective directions due to their anisotropic nature which makes the technique effective. UT operates in three detection modes, that is, reflection, transmission and backscattering of pulsed elastic waves in a material system.¹⁷ It introduces guided high-frequency sound waves (ranging from 1 kHz to 30 MHz⁴) to effectively detect flaw size, crack location, delamination location,⁸⁰ fibre waviness,³¹ meso-scale ply fibre orientation⁸¹ and layup stacking sequence.⁸²

Table 1. Summary of suppliers of devices and systems used for the acoustic emission-based NDT technique.

Supplier	Resolution (bit)	Dynamic range (dB)	Bandwidth (MHz)	Sampling speed (MHz)	Ref.
Physical Acoustics Co.	16	100	0.001–1.2	5–20	Ramirez-Jimenez et al., ⁶⁹ Marec et al. ⁷⁰ and Sikdar et al. ⁷¹
Meggitt Endevco	–	100	0.002–1.0	–	Barré and Benzeggagh ⁶³
Soundwel Technology Co. Ltd	16	85	0.001–2.5	0.5–10	Cui et al. ⁷²
IPPT PAN	–	40	0.005–0.5	–	Schabowicz et al. ⁷³
Vallen Systeme	–	100	0.1–0.45	–	Svečko et al. ⁷⁴

NDT: non-destructive testing.

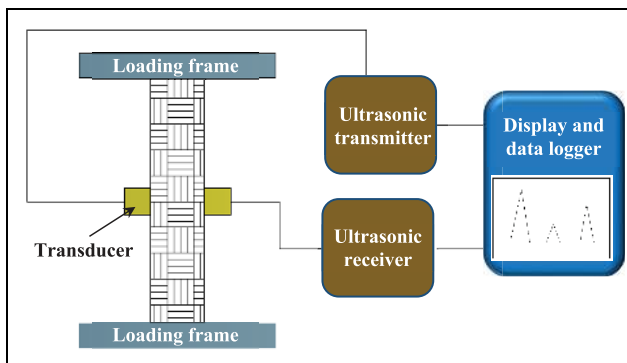
Please note the information in this table is incomplete, and not for advertising purposes – it should not be taken as endorsements by the authors.

Table 2. Summary of suppliers for the ultrasonic-based NDT technique.

Supplier	Resolution (bit)	Dynamic range (dB)	Bandwidth (MHz)	Sampling speed (MHz)	Ref.
ZETEC Inc.	16	–	0.5–18	50 or 60	Sherafat et al. ⁸⁵
Inspection Technology Europe	16	90	0.1–30	50/160	Dong et al. ⁸⁶
Advanced Technology Group	12	80	1–22	100	Růžek et al. ⁸⁷
Peak NDT	16	60	0.001–40	10–100	Riise et al. ⁸⁸
Olympus	–	60	0.2–20	–	Kim et al. ⁸⁹
Polytec Co.	14	–	0–25	–	Derusova et al. ⁹⁰

NDT: non-destructive testing.

Please note the information in this table is incomplete, and not for advertising purposes – it should not be taken as endorsements by the authors.

**Figure 6.** Principle of ultrasonic testing a composite material in transmission mode.

There are various types of UT systems with hundreds of guided wave modes and frequencies being available.⁷⁸ A typical UT system consists of a transmitter and receiver circuit, transducer tool and display devices, see Figure 6. The transmitter can either be arranged at an angle to the sample or in the form of phased array.⁸³ The guided Lamb waves can be generated using (1) ultrasonic probe, (2) laser, (3) piezoelectric element, (4) interdigital transducer or (5) optical fibre.⁸⁴ Table 2 provides some suppliers of UT equipment which may be applied to composites research.

The potential types of damage that guided Lamb wave-based NDT can provide are summarised by Rose,⁷⁷ the mode selection, generation and collection, modelling and simulation, signal processing and interpretation have been well documented by Su et al.⁸⁴ A later review on guided waves for damage identification in pipeline structures is provided by Guan et al.⁹¹ UT techniques for composites have been standardised: ASTM E2373⁹² gives the requirements for developing a time-of-flight (TOF) UT examination; ASTM E2580⁹³ for inspections on flat composite panels and sandwich structures in aerospace applications; ASTM E2981⁹⁴ for filament-wound pressure vessels in aerospace applications.

IRT

IRT is a method used to detect and process infrared energy emissions from an object by measuring and mapping thermal distributions.⁹⁵ Infrared energy is electromagnetic radiation with wavelengths longer than visible light, see Figure 3. The discovery of thermal radiation dated back to the early 1800s.⁵² Every object with a temperature higher than absolute zero emits electromagnetic radiation that falls into the infrared spectrum.⁹⁶ IRT has undergone rapid development in the last 30 years with developments in infrared cameras, data acquisition and processing techniques. It provides capabilities in terms of non-contact, non-invasive, real-time measurement, high resolution and covering large volumes.⁹⁷

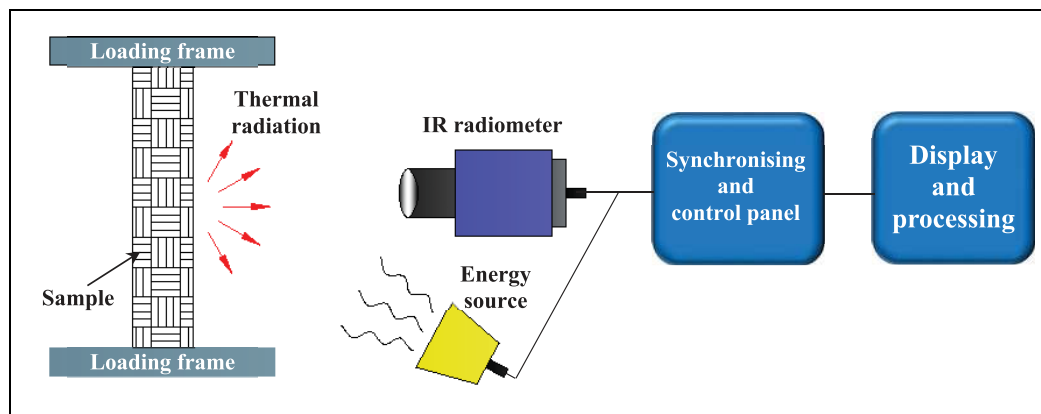
The IRT method is effectively used to monitor the entire life of a product, from manufacturing (on-line process control), to the finished product (NDT evaluation) and to in-service maintenance and diagnostics.⁵² It has been applied to research and various aspects within the industry, including NDT,⁹⁸ building diagnostics,⁹⁹ adhesion science,⁵² condition monitoring,¹⁰⁰ predictive or preventive maintenance,¹⁰¹ medical diagnostics,¹⁰² veterinary medicine¹⁰³ and many more. As for composite materials and structures, IRT-based NDT has also been widely used, especially during manufacturing for aerospace applications. It is used to detect inclusions, debonding, delamination and cracked networks.²⁷ Both Boeing and Airbus have used IRT for structural health monitoring to ensure the integrity of their composite products.⁹⁷

A typical IRT system contains an infrared radiometer, with/without energy source, synchronising and control panel, display software, see Figure 7. The radiometer is the core of the IRT system; it absorbs IR energy emissions and converts them into electrical voltage or current signals. They are then transmitted and displayed as infrared images of temperature distribution.⁵² The use of IRT can be implemented through (1) passive and (2) active thermography (AT).¹⁰⁴ In passive thermography (PT), thermal radiation is directly

Table 3. Summary of commercial infrared thermography systems and their key parameters applied to composite research.

Supplier	Spatial resolution (mrad)	Thermal sensitivity (mK)	Imaging resolution (pixel ²)	Imaging rate (fps)	Ref.
Thermal Wave Imaging Inc.	1.13	25	320 × 256	60	Avdelidis et al. ¹⁰⁷ and Chatterjee et al. ¹⁰⁸
Thermoteknix System Ltd.	0.47	70	384 × 288	50 or 60	Bolu et al. ¹⁰⁹
Fluke Corporation	0.93	50	640 × 480	9 or 60	Hu et al. ¹¹⁰
InfraTec GmbH	0.08–1.3	20	640 × 512	1–100	Jorge Aldave et al. ¹¹¹
Mikron Infrared	1.0	80	320 × 240	9 or 50	Naderi et al. ¹¹²
Optris	–	130	382 × 288	80	Bailey and Lafferty ¹¹³
NEC Avio	0.87	50	320 × 240	60	Vavilov et al. ¹¹⁴
FLIR System	0.19–1.36	20	320 × 256	50	Usamentiaga et al. ¹¹⁵ and Meola and Carlomagno ¹¹⁶

Please note the information in this table is incomplete, and not for advertising purposes – it should not be taken as endorsements by the authors.

**Figure 7.** Schematic of the measurement principles for an infrared thermography system in reflection mode.

emitted from surfaces of the test body under natural conditions and subsequently monitored. For AT, a heating or cooling flow is generated and propagated into the test object, and thermal responses according to the Stefan–Boltzmann law are then detected and recorded to reveal internal structures. Recent advances in signal processing techniques and equipment developments have made the AT method more practical and effective than the conventional PT approach.^{105,106} Table 3 gives some suppliers of IRT equipment which may be applied to composites research.

Based on energy stimulation methods, the AT method has developed into different categories. First, optical thermography is the most traditional form of IRT, using optical sources such as photographic flashes, halogen lamps or lasers, which are also known as pulsed thermography,¹¹⁷ modulated (lock-in) thermography¹¹⁸ or laser thermography,^{119,120} respectively. Second, induction thermography, which shares similar principles to ECT, that uses electronic or magnetic currents to induce energy waves.^{121–124} Third, mechanical thermography, which uses mechanical waves to interact

with internal structures to detect thermal waves from defects;¹²⁵ it can be implemented through vibrothermography,^{126,127} microwave thermography^{128,129} or ultrasonic lock-in thermography¹³⁰ which attracts increasing interest. Yang and He¹³¹ have presented a comprehensive review of the optical and non-optical IRT methods and their NDT applications in composite materials/structures. The reader is referred to ASTM E2582¹³² for standard practice on using IRT with composite panels and repair patches in aerospace applications.

THz testing

THz waves lie within the electromagnetic spectrum from 100 GHz to 30 THz,¹³³ which belong to non-ionising radiation and are not harmful to biological tissues (Figure 3). There are many THz wave sources in nature, although previously it has been difficult to generate and detect THz waves, so for many years, there have been few applications.¹³⁴ Due to breakthroughs in ultrafast lasers and ultra-micro machining technologies

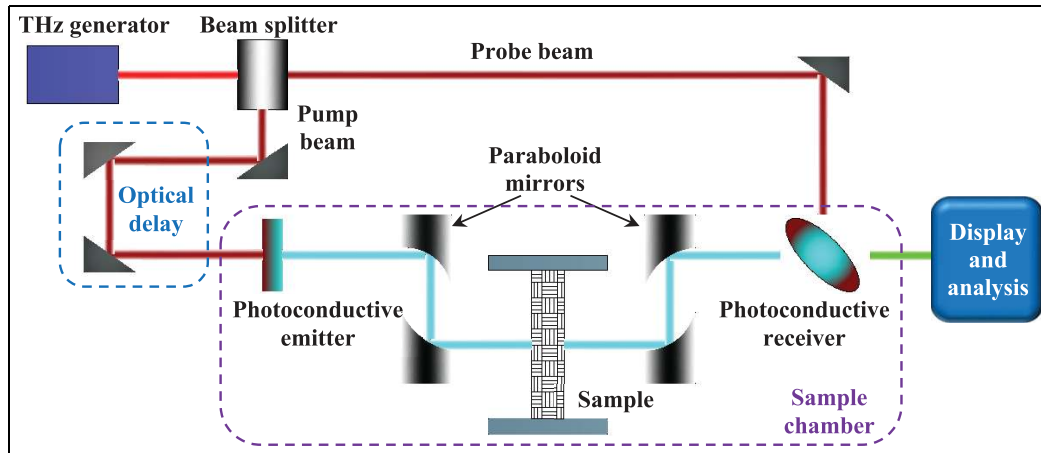


Figure 8. Schematic showing the measurement principles of THz time-domain spectroscopy using photoconductive antennas.

Table 4. Summary of terahertz-based NDT system suppliers.

THz supplier	Setup	Resolution (bit)	Dynamic range (dB)	Scanning range (mm ²)	Spectrum band (THz)	Ref.
Virginia Diodes Inc.	THz-CW	–	110	100 × 100	0.05–1.0	Dobroiu et al. ¹³⁷
Zomega Terahertz Co.	THz-TDS	–	70	150 × 150	0.1–4.0	Redo-Sanchez et al. ¹³⁹ and Wang et al. ¹⁴⁰
TeraView	THz-TDS	16	95	150 × 150	0.06–3.0	Dong et al. ¹⁴¹
TeraSense	THz-CW	16	–	128 × 64	0.05–1.0	Zhang et al. ¹⁴²
MenloSystems	THz-TDS	18	90	150 × 150	0.1–4.0	Han and Kang ¹⁴³
Toptica Photonics	THz-CW	–	100	100 × 100	0.1–6.0	Yahng et al. ¹⁴⁴
Luna Ltd.	THz-TDS	16	95	–	0.1–2.0	Zhang et al., ¹⁴⁵ Lopato ¹⁴⁶ and Okano and Watanabe ¹⁴⁷

NDT: non-destructive testing; THz: terahertz; CW: continuous wave; TDS: time-domain spectroscopy.

Please note the information in this table is incomplete, and not for advertising purposes – it should not be taken as endorsements by the authors.

during the 1980s,^{135,136} there has been a rapid expansion in applications for THz science and technology.⁴⁶ THz-based NDT technology has also started to be a promising technique for composite inspections,^{2,47} offering advantages in terms of higher resolution and better penetration in most materials compared to other techniques.¹³⁷

THz waves have good penetrating power for non-metallic, non-polar materials, including foams, ceramics, glass, resin, paint, rubber and composites. THz-based NDT techniques use the wave characteristics to detect, analyse and evaluate material systems, which has attracted wide interest in various fields, leading to rapid expansion.¹³⁸ Figure 8 shows an example of a typical setup of the THz-based NDT method, presenting the basic measuring principles in transmission mode.⁴⁵ The system induces THz short waves into a material, which interact with different phases, inclusions, defects or damage. Internal structures within the material are determined by detection and analysis of reflected or transmitted THz waves. Therefore, the

multi-phase and multi-layered nature of composites are well-suited to THz-based NDT – it offers multi-scale, more comprehensive information to detect and reveal internal structures and damage within a composite.⁴⁷

The THz-based NDT technique is usually implemented through (1) a THz time-domain spectroscopy system (THz-TDS), also known as pulsed spectroscopy, or (2) a continuous wave (THz-CW) system. The detection setup determines how information is evaluated within composite materials. In the THz-TDS system, short-pulsed THz waves are generated by optical excitation of a photoconductive antenna using a laser pulse emitting in the femtosecond regime,¹³³ the time-dependent evolution of the THz electric field of a single pulse is measured, which can be used to determine phase information within a composite. For the THz-CW system, high-power THz waves are produced through gas lasers, quantum cascade lasers or parametric sources² and phase information is measured by recording the average intensity (related to the amplitude of the wave) of the electromagnetic field. Table 4 shows some of the

Table 5. Summary of commercialised shearography system suppliers, and their key parameters applied to composite research.

Supplier	Inspection area (m ²)	Imaging resolution (pixel ²)	Imaging rate (Hz)	Ref.
Dantec Dynamics	0.01–2	1392 × 1040	10	Růžek et al. ⁸⁷ and Kadlec and Růžek ¹⁸⁶
ZEISS Optotechnik	–	220 × 160	–	Ibrahim et al. ¹⁸⁷
Optonor AS	0.01–4	1936 × 1216	–	Bisle et al. ¹⁸⁸ and Vollen et al. ¹⁸⁹
isi-sys GmbH	–	2560 × 1920	–	Pickering and Almond ¹⁹⁰ and Ochoa et al. ¹⁹¹
Laser Optical Engineering Ltd.	0.49	1280 × 1024	12	Francis et al. ¹⁷⁷
Laser Technology Inc.	0.01–0.05	1628 × 1236	30	Tyson and Newman ¹⁹²

Please note the information in this table is incomplete, and not for advertising purposes – it should not be taken as endorsements by the authors.

commercialised THz-based NDT systems and their key parameters. As an emerging NDT technique, standardised practice on using the THz approach is still developing.

There have been several reviews regarding applications of the THz-based technique, focusing on different aspects: Dhillon et al.⁴⁶ presented a comprehensive review on the roadmap of THz science and technology; Jansen et al.¹⁴⁸ reviewed progress and applications of THz systems in the polymer industry; Amenabar et al.² summarised the detection and imaging methods using THz waves, as well as their applications in composites; Zhong⁴⁷ further summed up the most recent advances.

Shearography

Shearography testing (ST) is a laser-based non-contact NDT technique, using a full-field speckle shearing interferometric method to overcome the limitations of holography testing.⁴⁹ This technique was first described and applied by Leendertz¹⁴⁹ and Leendertz and Butters¹⁵⁰ in the 1970s. To date, it has been used in various fields as a practical quantitative inspection tool to detect flaws and defects,^{151–153} leakage,¹⁵⁴ delamination and damage,^{155,156} as well as measurement of displacement and strain,^{157,158} curvature,^{159–162} residual stress,^{163–165} mechanical analysis,^{166,167} surface profiling¹⁶⁸ and dynamic vibration.^{169–171}

A typical shearography setup is shown in Figure 9. A laser beam illuminates a sample surface, and the beam is then scattered and reflected. The resulting speckle pattern is imaged through a shearing device (Michelson interferometer or diffractive optical element), which divides it into two coherent images with one being monitored during deformation. A controlled stressing process is essential and is applied through thermal,^{172,173} vacuum,^{163,174} vibration,¹⁵³ microwave¹⁷⁵ or mechanical loading.¹⁷⁶ The interferometric pattern is then captured and recorded by a charge-coupled device (CCD) camera, which results in a fringe pattern that contains structural information.¹⁷⁷ It has

been adopted for inspection and evaluation in various composite products, for example, pipes,^{178,179} sandwich structures,^{16,17,180} wind turbine blades,¹⁸¹ aerospace structures,^{182–184} as well as racing tyres.¹⁸⁵ An example of standard practice using shearography for polymer composites and sandwich core materials in aerospace is represented by ASTM E2581.¹⁸⁰ Some suppliers of commercialised shearography systems are given in Table 5.

DIC

DIC is a simple and cost-effective optical NDT technique for measuring strain and displacement, which are critical parameters within engineering and construction projects. It was developed in the 1980s¹⁹³ and has become widely used only in recent years due to the rapid development of computers and image acquisition methods. Images are usually captured through CCD cameras, possibly with the aid of microscopy. The DIC system tracks blocks of random pixels on a sample surface and compares digital photographs at different stages of deformation to build up full-field two-dimensional (2D) or three-dimensional (3D) deformation vector fields and strain maps.¹⁹⁴ Thus, any changes in the structure or surface can easily be reflected to give details on surface strain, deformation or crack propagation, making it ideal for studies of crack propagation and deformation. It offers more accurate strain monitoring than conventional extensometers or strain gauges, which often suffer from imperfect attachment to the measured surface and the limitations imposed by values that are averaged over the gauge length.¹⁹⁵

Figure 10 shows a typical DIC system for strain mapping of a composite sample; here, special illumination may be required. The sample is sprayed with a white stochastic speckle pattern prior to testing and two CCD cameras need to be calibrated each time. Imaging data can be analysed through commercialised software to reveal changes in speckle with reference images and strain or deformation can be calculated during the tests.

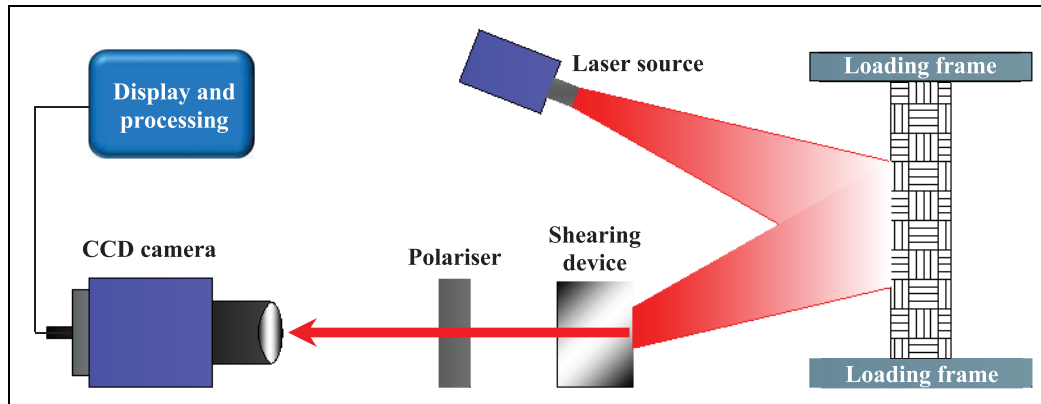


Figure 9. Schematic illustration of a shearography system.

Table 6. Summary of suppliers of DIC systems and their key parameters applied to composite research.

DIC supplier	Hardware/software	Imaging resolution (pixel ²)	Precision (μm/pixel)	Strain mapping	Ref.
Correlated solutions	Yes/yes	2240 × 1680	–	2D and 3D	Camirero et al. ²⁰⁰
Limess	Yes/yes	4096 × 3068	1.0	2D and 3D	Willems et al. ²⁰¹
Dantec Dynamics	Yes/yes	2560 × 1920	5.0	2D and 3D	Elhajjar and Shams ²⁰²
GOM	Yes/yes	4096 × 3068	4.8	2D and 3D	Catalanotti et al., ²⁰³ Dias et al. ²⁰⁴ and Furtado et al. ²⁰⁵
LaVision	Yes/yes	2240 × 1680	5.86	2D and 3D	Smyl et al. ²⁰⁶
Instron	Yes/yes	1280 × 720	1.0	2D	Sarasini et al. ²⁰⁷
MatchID	No/yes	–	–	2D and 3D	Wang et al. ²⁰⁸
isi-sys GmbH	Yes/no	1920 × 1200	2.0	2D and 3D	Manzato et al. ²⁰⁹

DIC: digital image correlation; 2D: two-dimensional; 3D: three-dimensional.

Please note the information in this table is incomplete and not for advertising purposes – it should not be taken as endorsements by the authors.

Thus, quality of the speckle pattern is vital for accuracy and precision in the DIC technique.¹⁹⁶ Pan¹⁹⁷ presented the historic developments, recent advances and future of DIC for surface deformation measurement; Hild et al.¹⁹⁸ discussed the capabilities of DIC in damage measurements; Aparna et al.¹⁹⁹ summarised studies on fatigue testing of composites using the DIC technique. Therefore, they are not elaborated here. Table 6 summarises some suppliers of DIC systems and certain examples in the literature. Audiences are recommended to refer to each supplier for full details.

Given the flexibility and versatility of DIC systems, standardisation of the DIC technique is difficult or even impossible to be applicable to each individual situation.¹⁹⁷

Imaging techniques

Imaging techniques refer to the NDT methods that are based on phase-contrast imaging, which were first developed in the 1930s.²¹⁰ They enable high-resolution imaging (a few angstroms), making it possible to

distinguish features at atomic or molecular levels. Developments in digital imaging technology and synchrotron radiation facilities have promoted the use of imaging techniques since the 1990s.²¹¹ To date, it has been reported that XRI is carried out either through lab-based X-ray tubes or synchrotron light sources; alternatively, NI uses neutrons generated from fission reactors or spallation sources.²¹² Both X-ray and neutron radiography have developed to be indispensable tools in various research fields ranging from solid matter to soft tissues.²¹¹

Synchrotron X-ray and neutron radiation are NDT techniques that provide insights into micro-structures, residual stress, strain and stress fields, crystallographic textures and so on, at atomic and crystalline levels. Their measurement and detection principles are similar, mainly depending on scattering techniques, see Figure 11. The incident light beams (monochromatic or white) are directed onto a sample, the scattered beams are captured by the detectors as a function of momentum transfer and/or transferred energy ΔE .²¹³ Diffraction patterns from a material in (a) can

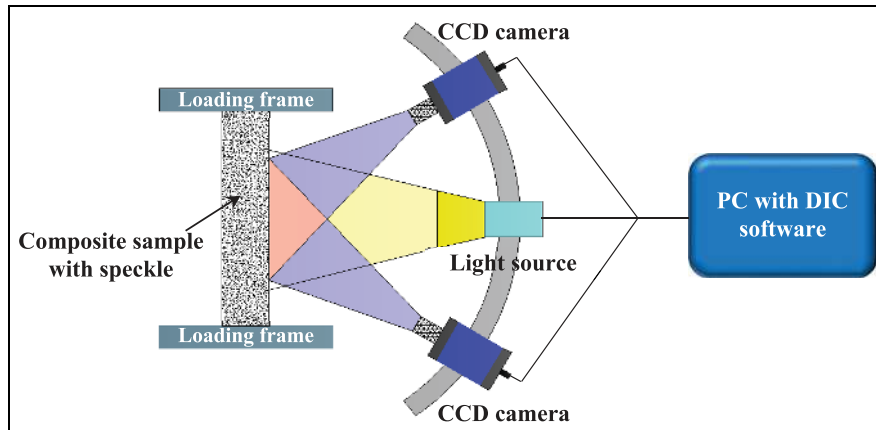


Figure 10. Schematic of a typical stereo-DIC setup for strain mapping of a composite sample sprayed with stochastic speckle pattern.

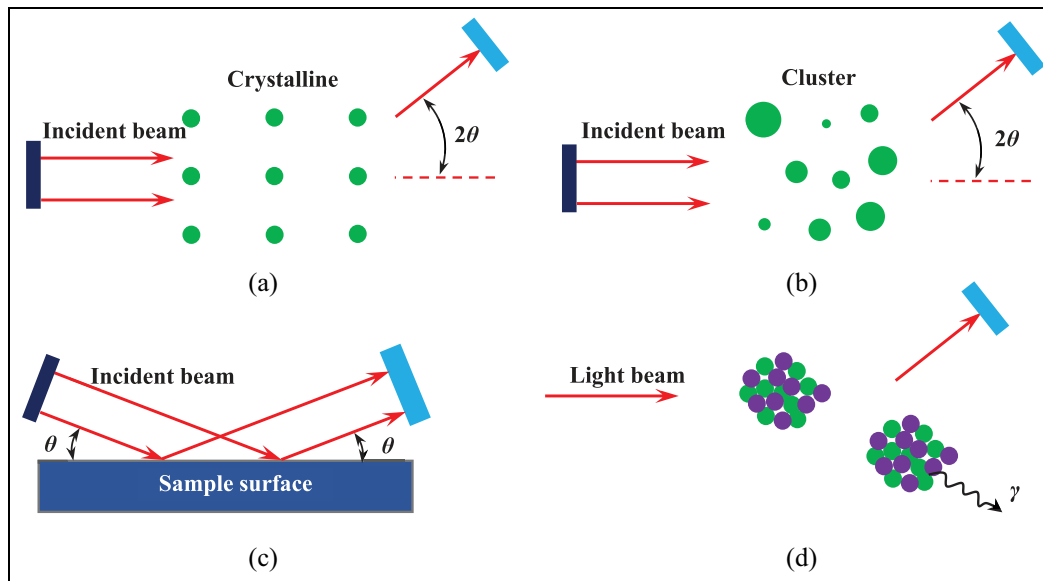


Figure 11. Schematic of synchrotron and neutron measurement techniques: (a) diffraction, (b) small-angle scattering, (c) reflectometry and (d) spectroscopy.

be used to characterise the crystalline structure, residual stress and crystallographic textures; in (b), small-angle scattering (SAS) uses smaller scattering angles than (a) to investigate material structures with various substances to provide quantitative statistical information at nanoscale levels; in (c), reflectometry is used to study the surface morphology of thin films or multi-layered composites and so on;²¹⁴ in (d), spectroscopy is performed to determine electronic, vibrational or magnetic excitations and diffusional processes in solids and liquids.

Although synchrotron and NI share basic principles, the neutron technique is superior in terms of penetration depth; that is X-rays (photons) can only be used non-destructively for examination in the near-surface regions.²¹⁵ Neutrons carry no electric charge, so there

is no electrostatic interaction with the electron cloud of an atom.²¹³ The characterisation and analysis of residual stresses in materials science using synchrotron and neutron radiation has been documented by Fitzpatrick and Lodini,²¹³ and Hutchings et al.²¹⁶ Also Banhart et al.²¹² have reviewed the applications of X-ray and NI to materials science and engineering.

XRI. A commonly used laboratory-based X-ray source for imaging is the X-ray tube, as schematically illustrated in Figure 12. A bias voltage of 30–60 kV is applied between the filament and metallic target in an evacuated X-ray tube, causing electrons emitted from the filament to collide with the metallic target at high

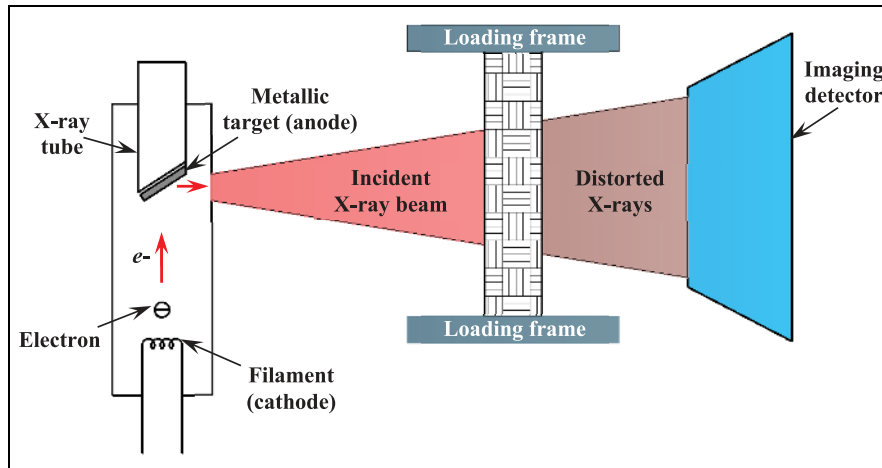


Figure 12. Schematic representation of laboratory-based X-ray imaging.

velocity (energy) and radiate X-rays. The wavelengths of the X-rays are about 0.5–2.5 Å and depend on the target material. The most commonly used metallic target is copper, which emits strong X-rays with a wavelength of 1.54 Å.²¹⁷ Laboratory XRI systems are usually cheaper and easier to access and are suitable for materials with higher phase contrast, such as glass fibre-reinforced composites. The acquisition time for laboratory XRI ranges from minutes at low resolution (sub-millimetre) to hours or even days at high resolution (sub-micron).²¹⁸

A major disadvantage of laboratory XRI systems is the lack of capability to penetrate deeply into engineering materials, which depends on X-ray energy and wavelength.²¹⁶ Although gamma-rays have higher penetrating capacity than X-rays, they are usually generated from a radioactive source, which cannot be turned off and is difficult to adopt as a compact source to provide a photon flux comparable to an X-ray tube; thus, detection efficiency is fairly low and long measuring times are required.²¹⁹

The limitations on penetration depth have been overcome by the rapid development of synchrotron facilities. Laboratory X-ray sources produce polychromatic and divergent X-ray beams, while a synchrotron X-ray beam is parallel, monochromatic, more coherent, with higher orders of flux and brightness. These factors determine the image quality and acquisition time. A synchrotron XRI system offers much higher levels of both signal-to-noise ratio and phase contrast, which makes it superior for low contrast materials, such as carbon fibre-reinforced composites. The high flux and brilliance of the X-ray beam allow very fast imaging acquisition with high resolution; for example, 1 tomogram per second with 1.1 μm spatial resolution using the TOMCAT beamline at the Swiss Light Source facility.²²⁰

Synchrotron facilities have gone through four generations of technical evolution. The first-generation synchrotron facility was built in the United States in 1946 and was primarily used for high-energy particle physics. The second-generation synchrotrons were dedicated to the production of synchrotron light in the 1980s, which used bending magnets to generate synchrotron light. The third-generation light sources originated in the 1990s,²²¹ with facilities that used insertion devices (wigglers and undulators) to produce intense and tuneable X-ray beams. The fourth-generation facilities will be based on free electron lasers which offer more advanced capabilities to generate brighter light sources.²²² Currently, there are about 50 synchrotron facilities around the world, supporting various investigations in engineering, health and medicine, materials science, chemistry, cultural heritage, environmental science and many more.^{222–231} Table 7 summarises the third- and fourth-generation synchrotron light source facilities throughout the world. Given that the first third-generation synchrotron facilities were built in 1993, some will be subjected to upgrading in the near future.²³¹

XRI can also be implemented through different methods as recently presented by Liu et al.,²¹⁰ Garcea et al.²¹⁸ reviewed the applications of X-ray computed tomography (CT) to polymer composites. Standard practice in using computed radiography (X-rays or γ-rays) for metallic and non-metallic materials is recommended in ASTM E2033;²³² ASTM E2662²³³ provides guidance on the radiographic examination of flat composite panels and sandwich core materials for aerospace applications.

NI. The neutron was discovered by Sir J Chadwick²³⁴ at Cambridge in 1932 through the collision of beryllium by α-particles from polonium. Neutrons have a wave

Table 7. Summary of third- and fourth-generation synchrotron light sources in operation and under construction worldwide.

Country	Location	Source	Energy (GeV)	Brilliance	Circumference (m)	Beamlines	Operation year/status
United States	Berkeley	ALS	1.9	10^{19}	196.8	40	1993
Italy	Basovizza	ELETTRA	2.0/2.4	10^{19}	259.2	28	1994
France	Grenoble	ESRF	6.0	10^{19}	844	56	1994
China	Taiwan	TLS	1.5	10^{17}	120	25	1994
Korea	Pohang	PLS	3.0	10^{20}	281.82	36	1995
United States	Lemont	APS	7.0	10^{14}	1104	68	1995
Japan	Hyogo	SPing8	8.0	10^{20}	1436	62	1997
Germany	Berlin	BESSY II	1.7	10^{19}	240	46	1999
Canada	Saskatoon	CLS	2.9	10^{20}	171	22	1999
Switzerland	Villigen	SLS	2.4	10^{20}	288	16	2001
United States	Menlo Park	SPEAR3	3.0	10^{20}	234	30	2004
United Kingdom	Didcot	DLS	3.0	10^{20}	561.6	39	2006
France	Saint-Aubin	SOLEIL	2.75	10^{19}	354	29	2006
Australia	Clayton	AS	3.0	10^{12}	216	10	2007
China	Beijing	BEPC II	2.0	10^{13}	240	14	2008
Germany	Hamburg	PETRA III	6.0	10^{21}	2304	21	2009
China	Shanghai	SSRF	3.5	10^{20}	432	31	2009
Spain	Barcelona	ALBA	3.0	10^{20}	268.8	9	2012
United States	Upton	NLS-II	3.0	10^{21}	792	28	2014
China	Taiwan	TPS	3.0	10^{21}	518.4	7	2016
Krakow	Poland	SOLARIS	1.5	10^{18}	96	2	2016
Jordan	Allan	SESAME	2.5	10^{18}	133	7	2017
Germany	Scheneffeld	XFEL	17.5	10^{33}	1700	6	2017
United States	Ithaca	CHESS-U	6.5	10^{21}	768.4	11	2018
Sweden	Lund	MAX IV	3.0	10^{22}	528	17	2019
France	Grenoble	ESRF-EBS	6.0	10^{21}	844	8	Under construction
Brazil	Campinas	SIRIUS	3.0	10^{21}	518.4	13	Under construction
China	Beijing	HEPS	6.0	10^{22}	1360	14	Under construction

Brilliance (brightness) is shown in photons/s/mrad²/mm²/0.1%bw.

character, their wavelengths are in the order of interatomic distances (~ 0.1 nm) and kinetic energies close to atomic vibration energies ($\sim 10^{-2}$ eV). Thus, they give rise to the possibilities of diffraction and inelastic scattering studies, which were experimentally demonstrated in 1946 by Wollan and Clifford using the Graphite Reactor at Oak Ridge National Laboratory, in the era of the Manhattan Project in the United States.²¹³ Important progress was made on neutron strain scanning (NSS) during the 1960s and 1970s. Techniques such as small-angle neutron scattering (SANS), neutron TOF scattering, backscattering or spin-echo techniques and neutron reflectivity subsequently broadened the applications of NSS to larger scientific domains such as solid-state chemistry, liquids, soft matter, materials science, geosciences and biology.²³⁵

A schematic example of NSS using ENGIN-X (ISIS Neutron and Muon Source, Rutherford Appleton Laboratory, UK) is presented in Figure 13.²³⁶ The pulsed neutron beam with a wide range of energy travels to the sample and, being scattered, the detectors then collect the diffracted neutrons at a fixed angle of $2\theta_b$. As neutrons can penetrate deeply into composite materials, strain/stress can be non-destructively measured.²³⁷ Neutrons are difficult and expensive to

produce – neutron sources are usually generated through either nuclear fission reactors (continuous neutron sources) or neutron spallation (pulsed neutron sources). Neutron source facilities are summarised chronologically in Table 8.^{213,238,239}

NI has progressed as a reliable NDT technique, in the forms of neutron topography and radiography;

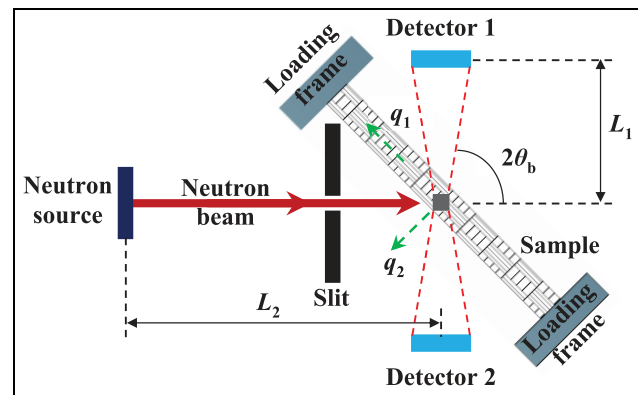


Figure 13. Schematic representation of a time-of-flight neutron strain scanner at the ENGIN-X. The elastic strain is measured along with the directions of the impulse exchange vectors, q_1 and q_2 , through the two detectors.

Table 8. Summary of neutron source facilities worldwide and their basic parameters.

Country	Location	Source	First open	Power (MW)	Flux (10^{14} n/cm ² /s)	Scattering instruments	Operating time (days/year)
Continuous neutron sources							
Canada	Chalk River	NRU	1957	120	3.0	6	300
Australia	Lucas Heights	HIFAR	1958	10	1.4	7	300
Hungary	Budapest	BNC	1959	10	1.6	7	200
Russia	Gatchina	WWR-M	1959	16	1.0	12	200
Denmark	Risø	DR3	1960	10	1.5	7	286
Sweden	Studsвик	R-2	1960	50	4.0	8	187
Japan	Tokai	JRR-3	1962	20	2.0	23	182
Germany	Juelich	FRJ-2	1962	23	2.0	16	200
Netherlands	Delft	HOR	1963	2	0.2	11	160
United States	Brookhaven	HFBR	1965	30	4.0	14	260
United States	Columbia	MURR	1966	10	6	4	338
Russia	Ekaterinburg	IVVW-2M	1966	15	2.0	6	250
United States	Oak Ridge	HFIR	1966	85	25.0	14	210
Norway	Kjeller	JEEP2	1967	2	0.22	8	269
United States	Gaithersburg	NBSR/NIST	1969	20	2.0	17	250
France	Grenoble	HFR-ILL	1972	58	12.0	32	225
Germany	Berlin	BER-2	1973	10	2.0	16	240
France	Saclay	Orphée	1980	14	3.0	25	240
Russia	Moscow	IR-8	1981	8	1.0	10	–
United States	Sacramento	MNRC	1990	2	0.1	5	50
Switzerland	Villigen	SINQ	1996	1	2.0	22	250
Korea	Taejon	Hanaro	1996	30	2.8	6	252
Australia	Lucas Heights	OPAL	2007	20	1.0	15	300
Pulsed neutron sources							
United States	Argonne	IPNS	1980	7	5	13	147
Japan	Tsukuba	KENS-KEK	1980	3 kW	3.0	16	80
Russia	Dubna	IBR2	1984	2	100	13	104
United Kingdom	Didcot	ISIS	1985	160 kW	20–100	28	141
United States	Los Alamos	LANSCE	1985	56	34	7	100
United States	Bloomington	LENS	2004	6 kW	0.001	3	–
United States	Oak Ridge	SNS	2006	1	1.5	19	240
Japan	Tokai	J-PARC	2007	1	0.8	1	–
China	Dongguan	CSNS	2018	0.1	0.01	18	Under construction
ERIC	Lund	ESS	2023	5	–	15	Under construction

specialised instrumentation at pulsed neutron sources includes RADEN@J-PARC²⁴⁰ and IMAT@ISIS.²⁴¹ Neutron tomography allows 2D or 3D imaging of the attenuation coefficient distribution within a material system; thus, internal structures and material composition can be visualised;²⁴² neutron radiography is a transmission imaging technique for heterogeneous materials, taking advantage of the scattering and/or absorption contrast between different elements.²⁴³

NI offers a typical spatial resolution of a few hundred microns²⁴⁴ and below 10 μm in the best case.²⁴⁵ Although XRI is able to provide sub-micron resolution, NI offers better sensitivity to light elements, especially hydrogen.²⁴⁵ In terms of efficiency, NI may take several hours (days) compared to minutes or even seconds for XRI; this is due to the low neutron flux, dependency on the number of slices/rotation steps and the materials under investigation. The fundamentals, instrumentation and early applications of NI are covered by Strobl

et al.,²⁴⁶ for recent advances and applications, refer to Kardjilov et al.²⁴⁷ and Woracek et al.²⁴⁵

Conclusions and outlook

NDT techniques are invaluable as tools for testing and evaluation, as may be required during various stages within the lifetime of a composite product. It is clear that each technique has its own potential but rarely achieves the capabilities for a full-scale diagnosis of possible defects and damage evolution in a composite system. Table 9 presents the benefits and limitations of the reviewed NDT methods. Appropriate selection of a suitable NDT technique can be challenging but is clearly essential to provide appropriate information for maintaining the structural integrity of composite materials and structures.

The applications and capabilities of each reviewed NDT technique for detection and evaluation of defects

Table 9. Benefits and limitations of established non-destructive testing techniques used in composite research.

NDT technique	Benefits	Limitations	Ref.
VI	Simple, rapid, low cost, easy handling	Only for surface flaws or damage Micro-defects are hardly detected Highly subjective, low repeatability and high reproducibility errors Multiple engineering approaches need to be applied for subsurface flaws	ASTM E298 ⁹⁴
AE	Provide real-time monitoring on growing flaws and damage Highly sensitive to stress waves Suitable for in situ and field tests Cover large measurement volumes	Specimen must be stressed Sensitivity is affected by surrounding noise Not suitable for thick specimen Difficult to interpret and characterise damage modes High cost of equipment and consumables High acquisition rates and measurements on test specimen are critical	Hamstad, ³ Scruby, ⁵⁴ Tensi ⁵⁶ and Dahmene et al. ⁵⁷
UT	Suitable for various material systems Able to detect, locate and size internal flaws Allows one-sided inspection Rapid scan and long-range inspection Good for assembly lines Compact and portable equipment, suitable for on-site inspection Often cost-effective Non-ionising radiation	Complex setup and transducer design Need skills and experience on multi-modes and complex features Sensitive to operational and environmental surroundings Hard to detect defects near probe Resolution may be limited by algorithms and computing power	Felice and Fan ⁷⁹ and Guan et al. ⁹¹
IRT	Real-time and large-field visual presentation of defects Suitable for wide selection of materials Allows one-sided inspection Safe and easy to operate Cost-effective and productive Non-ionising radiation	Vulnerable and sensitive for in situ and field tests Limited by cost and availability of excitation sources in the field Reduced accuracy with complex geometries Data processing is time-consuming; depends on computing power and algorithms Low speed of examination Restricted to nonconductive materials Costly	Bagavathiappan et al., ¹⁰⁰ Doshvarpassand et al., ¹⁰⁶ Jorge Aldave et al. ¹¹¹ and Vavilov and Burleigh ²⁴⁸
THz	Robust and repeatable, high scan rate with imaging High precision, sensitivity and resolution High penetration depths for most composites Non-ionising radiation		Amenabar et al., ² Zhong ⁴⁷ and Lopato ¹⁴⁶
ST	Non-contact and full-field surface strain measurement More resilient to environmental disturbance Suitable for large composite structures Efficient for high-speed, automated inspection in production environments	External excitation sources are required Limited tolerance to rigid-body motion Limited capabilities for subsurface damage detection Accuracy depends on various sources of uncertainties	Hung and Ho, ⁴⁹ Groves et al. ¹⁵⁸ and Francis et al. ¹⁷⁷
DIC	Cost-effective and easy implementation Adjustable spatial and temporal resolution Insensitive to ambient variations	Speckle patterns are required with high quality Accuracy depends on speckle pattern limited capability for subsurface detection	Dong and Pan ¹⁹⁶ and Pan ¹⁹⁷

(continued)

Table 9. Continued

NDT technique	Benefits	Limitations	Ref.
XRI	Suitable for various materials and in situ tests Can detect both surface and bulk defects 2D and 3D images reveal the very detailed shape of defects Special resolution at sub-micron level High efficiency Extensive image processing capability	Not suitable for large size structures Not suitable for in-field tests Access to both sides required Dangerous ionising radiation, requires protection Facilities and access are limited	Banhart et al., ²¹² Garcea et al. ²¹⁸ and Atsushi et al. ²⁴⁹
NI	Suitable for various materials and in situ tests Can detect both surface and bulk defects 2D and 3D images reveal the nature and detailed shape of defects Special resolution at the sub-millimetre level Extensive image processing capability Penetration depth greater than X-rays High sensitivity to light elements	Not suitable for in-field tests Access to both sides required Dangerous ionising radiation, requires protection Acquisition efficiency lower than XRI Facilities and access are limited and more expensive than XRI	Banhart et al., ²¹² Woracek et al. ²⁴⁵ and Kardjilov et al. ²⁴⁷

NDT: non-destructive testing; VI: visual inspection; AE: acoustic emission; UT: ultrasonic testing; IRT: infrared thermography; THz: terahertz; ST: shearography testing; DIC: digital image correlation; XRI: X-ray imaging; NI: neutron imaging; 2D: two-dimensional; 3D: three-dimensional.

and damage evolution in composite materials/structures are summarised in Table 10. As the volume and structural complexity of composite parts continue to grow, the uses of multi-NDT techniques are becoming increasingly popular in maintaining structural integrity; research in this approach is also growing rapidly.

The initial development and application of various NDT techniques are driven by demands from aerospace industries, which rapidly expand to other fields. AE, ultrasound, IRT, shearography, DIC and XRI represent the main techniques within composite industries and continue to play essential roles especially in aerospace, automotive, marine and construction applications. NDT techniques based on ultrasound, IRT and DIC are versatile and cost-effective solutions, which have been used extensively in many industrial fields, as well as academic research tools. THz waves can pass through opaque materials and detect internal defects and damage; thus, it is a promising NDT technique, possessing great potential in the near future. Innovation and development of compact and portable NDT devices will continue to have a major role for future NDT equipment as these will offer in-service or *in-situ* inspections to facilitate the decision-making process.

Considering the complex nature of defects and damage detection in composites, the future development of NDT techniques will increasingly depend on intelligent and automated inspection systems with high accuracy and efficiency in data processing. Machine learning and deep learning provide significant potential for the NDT evaluation of composite materials – artificial intelligence-based approaches offer fast decision-making without human interference. Various automated diagnostic systems have been proposed for different NDT techniques to offer fast and accurate analysis. These are achieved through artificial neural network coding or algorithms to enable automatic detection and recognition of defects/damage. Examples include applying pattern recognition to discriminate failure modes in composites using AE data,³⁰⁷ damage classification in carbon fibre-reinforced polymer (CFRP) laminates using artificial neural networks in UT,³⁰⁸ automatic defect detection through IRT in CFRP laminates³⁰⁹ and honeycomb composite structures,³¹⁰ an automated shearography system for cylindrical surface inspection using machining learning,²⁵² neural network-based hybrid signal processing for THz pulsed imaging.³¹¹ Despite the exciting achievements in NDT techniques, there is still substantial work required to develop fast and affordable systems for both equipment and data processing methods to promote their practical implementation in industry.

Although X-ray and NI are powerful tools for NDT tests offering super high resolution, both imaging techniques are based on ionising radiation, that is,

Table 10. Applications and capabilities of established NDT techniques for composite inspection and evaluation.

Defects/damages	AE	UT	IRT	THz	ST	DIC	XRI	NI
Manufacturing induced flaws/defects					Ye et al. ²⁵²		Senck et al. ²⁵³	
Surface defects	De Simone et al. ²⁵⁴	Ashir et al. ²⁵⁵ and Podymova et al. ²⁵⁶	Pracht and Swiderski ²⁵⁰ and Pracht and Swiderski ²⁵⁰ and Bendada et al. ²⁵⁷	Stoik et al. ²⁵¹ Dong et al. ¹⁴¹ Zhang et al. ¹⁴⁵ and Stoik et al. ²⁵¹	De Angelis et al. ¹⁵³ and Yang et al. ²⁵⁸		Centea and Hubert ²⁵⁹	Alam et al. ²⁶⁰ and Kam et al. ²⁶¹
Delamination	Saeedifar et al. ²⁶²	Laureti et al. ²⁶³	Laureti et al. ²⁶³	Ryu et al. ²⁶⁴	Pagliarulo et al. ²⁶⁵	Szebenyi and Hliva ²⁶⁶		
Location of depth/size	Marec et al. ⁷⁰	Ellison and Kim ²⁶⁷	Yi et al. ²⁶⁸	Dong et al. ⁸⁶	De Angelis et al. ¹⁵³		Ellison and Kim ²⁶⁷	
Interface debonding		Li and Zhou ²⁶⁹	Yi et al. ²⁷⁰	Dai et al. ²⁷¹			Wen et al. ²⁷²	
Fibre content and orientation		Pain and Drinkwater ³¹	Fernandes et al. ²⁷³	Dong et al. ¹⁴¹		Mendoza et al. ²⁷⁴	Prade et al. ²⁷⁵	Evans et al. ²⁷⁶
Cracks, fibre breakage/fracture	Dornfeld ²⁷⁷	Lee et al. ²⁷⁹	Garcia Perez et al. ²⁸⁰	Dong et al. ¹⁴¹	Yusuf et al. ¹⁸⁴	Catalanotti et al. ²⁰³	Hong et al. ²⁸¹	Zhang et al. ²⁸²
Moisture, liquids or voids	and Liu et al. ²⁷⁸		Safai and Wang ²⁸³	Federici ²⁸⁴	Tyson and Newman ¹⁵⁴		De Pairscau du Plessix et al. ²⁸⁵	Alam et al. ²⁸⁶ and Oromiehie et al. ²⁸⁷
Shape/surface profiling					Shang et al. ¹⁶⁸			
In-service in situ detection					Růžek et al. ⁸⁷	Ranatunga et al. ²⁹⁰	Ranatunga et al. ²⁹⁰	
Impact damage		Wang et al. ²⁸⁸	Růžek et al. ⁸⁷ and Wang et al. ²⁸⁸	Destic and Bouvet ²⁸⁹	Pieczonka et al. ¹⁵⁶ and Kadlec and Růžek ¹⁸⁶			
Tensile cracking/damage	Liu et al. ²⁷⁸ and Aslan ²⁹¹					Sarasini et al. ²⁰⁷	Sirinuk et al. ²⁹²	Sirinuk et al. ²⁹²
Compressive failure								
Bending fatigue damage	Djabali et al. ²⁹⁴					Yuan and Wang ²⁹³		
Tensile-tensile fatigue	Dia et al. ²⁹⁶			Lopato and Chady ²⁹⁵		Djabali et al. ²⁹⁴	Djabali et al. ²⁹⁴	
Structural damage monitoring	Aggelis et al. ²⁹⁹		Sfarra et al. ³⁰⁰	Rahani et al. ³⁰¹		Aparna et al. ¹⁹⁹ Arora et al. ³⁰²	Wagner et al. ²⁹⁷	Reid et al. ²⁹⁸
Quantitative strain monitoring					Anisimov and Groves ³⁰³	Elhajjar and Shams ²⁰²	Sui et al. ³⁰⁴	Wang et al. ²³⁷
Mechanical analysis					Lee et al. ^{166,167}	Smyl et al. ²⁰⁶		
Hygrothermal damage				Stoik et al. ³⁰⁵			Jiang et al. ³⁰⁶	

NDT: non-destructive testing; AE: acoustic emission; UT: ultrasonic testing; IRT: infrared thermography; THz: terahertz; ST: shearography testing; DIC: digital image correlation; XRI: X-ray imaging; NI: neutron imaging.

specimens have to be analysed using radiation facilities which are inconvenient compared to other NDT techniques. Also, locations and availability of synchrotron facilities are very limited, which further constrain their accessibility and costs. Portable X-ray or neutron generators have been commercialised to provide easier access. While they have found applications in aerospace, marine, construction and pipeline inspection, their capabilities for composite industries are limited. The use of NI depends on advances in neutron production and instrumentation, while its research community is growing rapidly. Free electron lasers and modern spallation sources are promising techniques that should enhance the future development of NDT technology towards more advanced capabilities.


Declaration of conflicting interests

The author(s) declared no potential conflicts of interest with respect to the research, authorship and/or publication of this article.

Funding

The author(s) received no financial support for the research, authorship and/or publication of this article.

ORCID iD

Bing Wang  <https://orcid.org/0000-0002-1480-3301>

References

- Ashby MF and Cebon D. Materials selection in mechanical design. *Le J Phys IV* 1993; 3: C7-1–C7-9.
- Amenabar I, Lopez F and Mendikute A. In introductory review to THz non-destructive testing of composite mater. *J Infrared Millim Terahertz Waves* 2013; 34: 152–169.
- Hamstad MA. A review: acoustic emission, a tool for composite-materials studies. *Exp Mech* 1986; 26: 7–13.
- Duchene P, Chaki S, Ayadi A, et al. A review of non-destructive techniques used for mechanical damage assessment in polymer composites. *J Mater Sci* 2018; 53: 7915–7938.
- ASTM E2533:2017. Standard guide for nondestructive testing of polymer matrix composites used in aerospace applications.
- Summerscales J. *Non-destructive testing of fibre-reinforced plastics composites*. Berlin: Springer, 1990.
- Birt EA and Smith RA. A review of NDE methods for porosity measurement in fibre-reinforced polymer composites. *Insight Nondestruct Test Cond Monit* 2004; 46: 681–686.
- Cheng L and Tian GY. Comparison of nondestructive testing methods on detection of delaminations in composites. *J Sensors* 2012; 2012: 408437.
- Heuer H, Schulze M, Pooch M, et al. Review on quality assurance along the CFRP value chain–non-destructive testing of fabrics, preforms and CFRP by HF radio wave techniques. *Compos Part B Eng* 2015; 77: 494–501.
- Li Z and Meng Z. A review of the radio frequency non-destructive testing for carbon-fibre composites. *Meas Sci Rev* 2016; 16: 68–76.
- Gholizadeh S. A review of non-destructive testing methods of composite materials. *Proced Struct Integr* 2016; 1: 50–57.
- Guo N and Cawley P. The non-destructive assessment of porosity in composite repairs. *Composites* 1994; 25: 842–850.
- Naebe M, Abolhasani MM, Khayyam H, et al. Crack damage in polymers and composites: a review. *Polym Rev* 2016; 56: 31–69.
- Asif M, Khan MA, Khan SZ, et al. Identification of an effective nondestructive technique for bond defect determination in laminate composites – a technical review. *J Compos Mater* 2018; 52: 3589–3599.
- Jolly MR, Prabhakar A, Sturzu B, et al. Review of non-destructive testing (NDT) techniques and their applicability to thick walled composites. *Proced CIRP* 2015; 38: 129–136.
- Hsu DK. Nondestructive evaluation of sandwich structures: a review of some inspection techniques. *J Sandw Struct Mater* 2009; 11: 275–291.
- Ibrahim ME. Nondestructive evaluation of thick-section composites and sandwich structures: a review. *Compos Part A Appl Sci Manuf* 2014; 64: 36–48.
- Cawley P. The rapid non-destructive inspection of large composite structures. *Composites* 1994; 25: 351–357.
- Mook G, Pohl J and Michel F. Non-destructive characterization of smart CFRP structures. *Smart Mater Struct* 2003; 12: 997–1004.
- Zou Y, Tong L and Steven GP. Vibration-based model-dependent damage (delamination) identification and health monitoring for composite structures – a review. *J Sound Vib* 2000; 230: 357–378.
- Tuloup C, Harizi W, Aboura Z, et al. On the use of in-situ piezoelectric sensors for the manufacturing and structural health monitoring of polymer-matrix composites: a literature review. *Compos Struct* 2019; 215: 127–149.
- Greene E. Marine composites non-destructive evaluation. *Sh Struct* 2014; 1: 416–427.
- Drewry MA and Georgiou GA. A review of NDT techniques for wind turbines. *Insight Nondestruct Test Cond Monit* 2007; 49: 137–141.
- Ciang CC, Lee JR and Bang HJ. Structural health monitoring for a wind turbine system: a review of damage detection methods. *Meas Sci Technol* 2008; 19: 122001.
- Raišutis R, Jasiūnienė E, Šlitteris R, et al. The review of non-destructive testing techniques suitable for inspection of the wind turbine blades. *Ultragarsas* 2008; 63: 26–30.
- Galappaththi UIK, De Silva AKM, Macdonald M, et al. Review of inspection and quality control techniques for composite wind turbine blades. *Insight Non-destruct Test Cond Monit* 2012; 54: 82–85.
- Garnier C, Pastor ML, Eyma F, et al. The detection of aeronautical defects in situ on composite structures

- using Non Destructive Testing. *Compos Struct* 2011; 93: 1328–1336.
28. Katnam KB, Da Silva LFM and Young TM. Bonded repair of composite aircraft structures: a review of scientific challenges and opportunities. *Prog Aerosp Sci* 2013; 61: 26–42.
 29. Fahr A. *Aeronautical applications of non-destructive testing*. Lancaster, PA: DEStech Publications, Inc., 2013.
 30. Joyce PJ, Kugler D and Moon TJ. A technique for characterizing process-induced fiber waviness in unidirectional composite laminates-using optical microscopy. *J Compos Mater* 1997; 31: 1694–1727.
 31. Pain D and Drinkwater BW. Detection of fibre waviness using ultrasonic array scattering data. *J Nondestruct Eval* 2013; 32: 215–227.
 32. Hull D and Clyne TW. *An introduction to composite materials*. Cambridge: Cambridge University Press, 1996.
 33. Wang B and Fancey KS. Viscoelastically prestressed polymeric matrix composites: an investigation into fibre deformation and prestress mechanisms. *Compos Part A Appl Sci Manuf* 2018; 111: 106–114.
 34. Wang J, Potter KD, Hazra K, et al. Experimental fabrication and characterization of out-of-plane fiber waviness in continuous fiber-reinforced composites. *J Compos Mater* 2012; 46: 2041–2053.
 35. Hyer MW. Some observations on the cured shape of thin unsymmetric laminates. *J Compos Mater* 1981; 15: 175–194.
 36. Hyer MW. The room-temperature shapes of four-layer unsymmetric cross-ply laminates. *J Compos Mater* 1982; 16: 318–340.
 37. Wang B and Fancey KS. A bistable morphing composite using viscoelastically generated prestress. *Mater Lett* 2015; 158: 108–110.
 38. Wang B, Ge C and Fancey KS. Snap-through behaviour of a bistable structure based on viscoelastically generated prestress. *Compos Part B Eng* 2017; 114: 23–33.
 39. Lubin G. *Handbook of composites*. Berlin: Springer, 2013.
 40. Berthelot JM and Rhazi J. Acoustic emission in carbon fibre composites. *Compos Sci Technol* 1990; 37: 411–428.
 41. Haque A and Hossain MK. Effects of moisture and temperature on high strain rate behavior of S2-glass-vinyl ester woven composites. *J Compos Mater* 2003; 37: 627–647.
 42. Huang S and Wang S. *New technologies in electromagnetic non-destructive testing*. Berlin: Springer, 2016.
 43. Ghoni R, Dollah M, Sulaiman A, et al. Defect characterization based on eddy current technique: technical review. *Adv Mech Eng* 2014; 6: 182496.
 44. Koyama K, Hoshikawa H and Kojima G. Eddy current nondestructive testing for carbon fiber-reinforced composites. *J Press Vessel Technol* 2013; 135: 41501.
 45. Ferguson B and Zhang XC. Materials for terahertz science and technology. *Nat Mater* 2002; 1: 26–33.
 46. Dhillon SS, Vitiello MS, Linfield EH, et al. The 2017 terahertz science and technology roadmap. *J Phys D Appl Phys* 2017; 50: 43001.
 47. Zhong S. Progress in terahertz nondestructive testing: a review. *Front Mech Eng* 2019; 14: 273–281.
 48. Ambrosini D and Ferraro P. Here, there and everywhere: the art and science of optics at work. *Opt Laser Eng* 2018; 104: 1–8.
 49. Hung YY and Ho HP. Shearography: an optical measurement technique and applications. *Mater Sci Eng R Reports* 2005; 49: 61–87.
 50. Yang L and Xie X. *Digital shearography: new developments and applications*. Bellingham, WA: SPIE Press, 2016.
 51. Arai M and Crawford K. Neutron sources and facilities. In: Anderson IS, McGreevy RL and Bilheux H. (eds) *Neutron imaging and applications*. Berlin: Springer, 2009, pp.13–30.
 52. Meola C and Carlomagno GM. Application of infrared thermography to adhesion science. *J Adhes Sci Technol* 2006; 20: 589–632.
 53. Schoonahd JW, Gould JD and Miller LA. Studies of visual inspection. *Ergonomics* 1973; 16: 365–379.
 54. Scruby CB. An introduction to acoustic emission. *J Phys E* 1987; 20: 946–953.
 55. Kaiser J. *An investigation into the occurrence of noises in tensile tests or a study of acoustic phenomena in tensile tests*. PhD Dissertation, Technische Hochschule Munchen, Munich, 1950.
 56. Tensi HM. The Kaiser-effect and its scientific background. *J Acoust Emiss* 2004; 22: s1–s16.
 57. Dahmene F, Yaacoubi S and Mountassir MEL. Acoustic emission of composites structures: story, success, and challenges. *Phys Procedia* 2015; 70: 599–603.
 58. Huguet S, Godin N, Gaertner R, et al. Use of acoustic emission to identify damage modes in glass fibre reinforced polyester. *Compos Sci Technol* 2002; 62: 1433–1444.
 59. Godin N, Huguet S, Gaertner R, et al. Clustering of acoustic emission signals collected during tensile tests on unidirectional glass/polyester composite using supervised and unsupervised classifiers. *NDT E Int* 2004; 37: 253–264.
 60. Kordatos EZ, Dassios KG, Aggelis DG, et al. Rapid evaluation of the fatigue limit in composites using infrared lock-in thermography and acoustic emission. *Mech Res Commun* 2013; 54: 14–20.
 61. Nechad H, Helmstetter A, El Guerjouma R, et al. Creep ruptures in heterogeneous materials. *Phys Rev Lett* 2005; 94: 45501.
 62. Chou HY, Mouritz AP, Bannister MK, et al. Acoustic emission analysis of composite pressure vessels under constant and cyclic pressure. *Compos Part A Appl Sci Manuf* 2015; 70: 111–120.
 63. Barré S and Benzeggagh ML. On the use of acoustic emission to investigate damage mechanisms in glass-fibre-reinforced polypropylene. *Compos Sci Technol* 1994; 52: 369–376.
 64. ASTM E1067:2018. Standard practice for acoustic emission examination of fiberglass reinforced plastic resin (FRP) tanks/vessels.
 65. ASTM E1118:2016. Standard practice for acoustic emission examination of reinforced thermosetting resin pipe (RTRP).

66. ASTM E2191:2016. Standard practice for examination of gas-filled filament-wound composite pressure vessels using acoustic emission.
67. ASTM E2076:2015. Standard practice for examination of fiberglass reinforced plastic fan blades using acoustic emission.
68. ASTM E2661:2015. Standard practice for acoustic emission examination of plate-like and flat panel composite structures used in aerospace applications.
69. Ramirez-Jimenez CR, Papadakis N, Reynolds N, et al. Identification of failure modes in glass/polypropylene composites by means of the primary frequency content of the acoustic emission event. *Compos Sci Technol* 2004; 64: 1819–1827.
70. Marec A, Thomas JH and El Guerjouma R. Damage characterization of polymer-based composite materials: multivariable analysis and wavelet transform for clustering acoustic emission data. *Mech Syst Signal Process* 2008; 22: 1441–1464.
71. Sikdar S, Mirgal P, Banerjee S, et al. Damage-induced acoustic emission source monitoring in a honeycomb sandwich composite structure. *Compos Part B Eng* 2019; 158: 179–188.
72. Cui X, Yan Y, Ma Y, et al. Localization of CO₂ leakage from transportation pipelines through low frequency acoustic emission detection. *Sens Actuat A Phys* 2016; 237: 107–118.
73. Schabowicz K, Gorzelańczyk T and Szymków M. Identification of the degree of degradation of fibre-cement boards exposed to fire by means of the acoustic emission method and artificial neural networks. *Materials* 2019; 12: 656.
74. Svečko R, Kusić D, Kek T, et al. Acoustic emission detection of macro-cracks on engraving tool steel inserts during the injection molding cycle using PZT sensors. *Sensors* 2013; 13: 6365–6379.
75. Vary A. Acousto-ultrasonic characterization of fiber reinforced composites. *Mater Eval* 1982; 40: 1–15.
76. Vary A. The acousto-ultrasonic approach. In: Duke J (ed.) *Acousto-ultrasonics*. Berlin: Springer, 1988, pp.1–21.
77. Rose JL. A baseline and vision of ultrasonic guided wave inspection potential. *J Press Vessel Technol* 2002; 124: 273–282.
78. Rose JL. *Ultrasonic guided waves in solid media*. Cambridge: Cambridge University Press, 2014.
79. Felice MV and Fan Z. Sizing of flaws using ultrasonic bulk wave testing: a review. *Ultrasonics* 2018; 88: 26–42.
80. Munian RK, Mahapatra DR and Gopalakrishnan S. Lamb wave interaction with composite delamination. *Compos Struct* 2018; 206: 484–498.
81. Smith RA, Nelson LJ, Mienczakowski MJ, et al. Ultrasonic tracking of ply drops in composite laminates. *AIP Conf Proc* 2016; 1706: 50006.
82. Smith RA and Clarke B. Ultrasonic C-scan determination of ply stacking sequence in carbon-fibre composites. *Insight Nondestruct Test Cond Monit* 1994; 36: 741–747.
83. Li C, Pain D, Wilcox PD, et al. Imaging composite material using ultrasonic arrays. *NDT E Int* 2013; 53: 8–17.
84. Su Z, Ye L and Lu Y. Guided Lamb waves for identification of damage in composite structures: a review. *J Sound Vib* 2006; 295: 753–780.
85. Sherafat MH, Quaegebeur N, Hubert P, et al. Experimental model of impact damage for guided wave-based inspection of composites. *J Nondestruct Eval Diagn Progn Eng Syst* 2018; 1: 40801.
86. Dong J, Kim B, Locquet A, et al. Nondestructive evaluation of forced delamination in glass fiber-reinforced composites by terahertz and ultrasonic waves. *Compos Part B Eng* 2015; 79: 667–675.
87. Růžek R, Lohonka R and Jironč J. Ultrasonic C-scan and shearography NDI techniques evaluation of impact defects identification. *NDT E Int* 2006; 39: 132–142.
88. Riise J, Mineo C, Pierce SG, et al. Adapting robot paths for automated NDT of complex structures using ultrasonic alignment. *AIP Conf Proc* 2019; 2102: 40006.
89. Kim H, Kim T, Morrow D, et al. Stress measurement of a pressurized vessel using ultrasonic subsurface longitudinal wave with 1–3 composite transducers. *IEEE Trans Ultrason Ferroelectr Freq Control* 2020; 67: 158–166.
90. Derusova DA, Vavilov VP, Sfarra S, et al. Applying ultrasonic resonance vibrometry for the evaluation of impact damage in natural/synthetic fibre reinforced composites. *Polym Test* 2018; 68: 70–76.
91. Guan R, Lu Y, Duan W, et al. Guided waves for damage identification in pipeline structures: a review. *Struct Control Health Monit* 2017; 24: e2007.
92. ASTM E2373:2014. Standard practice for use of the ultrasonic time of flight diffraction (TOFD) technique.
93. ASTM E2580:2017. Standard practice for ultrasonic testing of flat panel composites and sandwich core materials used in aerospace applications.
94. ASTM E2981:2015. Standard guide for nondestructive testing of the composite overwraps in filament wound pressure vessels used in aerospace applications.
95. Vollmer M and Möllmann KP. *Infrared thermal imaging: fundamentals, research and applications*. 2nd ed. Hoboken, NJ: John Wiley & Sons, 2017.
96. Meola C. *Infrared thermography recent advances and future trends*. Sharjah, UAE: Bentham Science Publishers, 2012.
97. Zhu YK, Tian GY, Lu RS, et al. A review of optical NDT technologies. *Sensors* 2011; 11: 7773–7798.
98. Usamentiaga R, Venegas P, Guerediaga J, et al. Infrared thermography for temperature measurement and non-destructive testing. *Sensors* 2014; 14: 12305–12348.
99. Balaras CA and Argiriou AA. Infrared thermography for building diagnostics. *Energ Build* 2002; 34: 171–183.
100. Bagavathiappan S, Lahiri BB, Saravanan T, et al. Infrared thermography for condition monitoring—a review. *Infrared Phys Technol* 2013; 60: 35–55.
101. Huda ASN and Taib S. Application of infrared thermography for predictive/preventive maintenance of thermal defect in electrical equipment. *Appl Therm Eng* 2013; 61: 220–227.
102. Lahiri BB, Bagavathiappan S, Jayakumar T, et al. Medical applications of infrared thermography: a review. *Infrared Phys Technol* 2012; 55: 221–235.

103. Soroko M and Howell K. Infrared thermography: current applications in equine medicine. *J Equine Vet Sci* 2018; 60: 90–96.
104. Wiecek B. Review on thermal image processing for passive and active thermography. In: *Proceedings of the 2005 IEEE engineering in medicine and biology 27th annual conference*, Shanghai, China, 17–18 January 2006, pp.686–689. New York: IEEE.
105. Theodorakeas P, Cheilakou E, Ftikou E, et al. Passive and active infrared thermography: an overview of applications for the inspection of mosaic structures. *J Phys Conf Ser* 2015; 655: 12061.
106. Doshvarpassand S, Wu C and Wang X. An overview of corrosion defect characterization using active infrared thermography. *Infrared Phys Technol* 2019; 96: 366–389.
107. Avdelidis NP, Hawtin BC and Almond DP. Transient thermography in the assessment of defects of aircraft composites. *NDT E Int* 2003; 36: 433–439.
108. Chatterjee K, Tuli S, Pickering SG, et al. A comparison of the pulsed, lock-in and frequency modulated thermography nondestructive evaluation techniques. *NDT E Int* 2011; 44: 655–667.
109. Bolu G, Gachagan A, Pierce G, et al. Reliable thermosonic inspection of aero engine turbine blades. *Insight Non-destruct Test Cond Monit* 2010; 52: 488–493.
110. Hu Q, Chen Y, Hong J, et al. A smart epoxy composite based on phase change microcapsules: preparation, microstructure, thermal and dynamic mechanical performances. *Molecules* 2019; 24: 916.
111. Jorge Aldave I, Venegas Bosom P, Vega González L, et al. Review of thermal imaging systems in composite defect detection. *Infrared Phys Technol* 2013; 61: 167–175.
112. Naderi M, Kahirdeh A and Khonsari MM. Dissipated thermal energy and damage evolution of glass/epoxy using infrared thermography and acoustic emission. *Compos Part B Eng* 2012; 43: 1613–1620.
113. Bailey PBS and Lafferty AD. Specimen gripping effects in composites fatigue testing—concerns from initial investigation. *Exp Polym Lett* 2015; 9: 480–488.
114. Vavilov VP, Plesovskikh AV, Chulkov AO, et al. A complex approach to the development of the method and equipment for thermal nondestructive testing of CFRP cylindrical parts. *Compos Part B Eng* 2015; 68: 375–384.
115. Usamentiaga R, Venegas P, Guerediaga J, et al. Feature extraction and analysis for automatic characterization of impact damage in carbon fiber composites using active thermography. *NDT E Int* 2013; 54: 123–132.
116. Meola C and Carlomagno GM. Infrared thermography to evaluate impact damage in glass/epoxy with manufacturing defects. *Int J Impact Eng* 2014; 67: 1–11.
117. Sun JG. Analysis of pulsed thermography methods for defect depth prediction. *J Heat Transf* 2006; 128: 329–338.
118. Busse G, Wu D and Karpen W. Thermal wave imaging with phase sensitive modulated thermography. *J Appl Phys* 1992; 71: 3962–3965.
119. Li T, Almond DP and Rees DAS. Crack imaging by scanning pulsed laser spot thermography. *NDT E Int* 2011; 44: 216–225.
120. Schlichting J, Maierhofer C and Kreutzbruck M. Crack sizing by laser excited thermography. *NDT E Int* 2012; 45: 133–140.
121. Riegert G, Zweschper T and Busse G. Lock-in thermography with eddy current excitation. *Quant Infrared Thermogr J* 2004; 1: 21–32.
122. Pan M, He Y, Tian G, et al. Defect characterisation using pulsed eddy current thermography under transmission mode and NDT applications. *NDT E Int* 2012; 52: 28–36.
123. He Y, Pan M and Luo F. Defect characterisation based on heat diffusion using induction thermography testing. *Rev Sci Instrum* 2012; 83: 104702.
124. Liang T, Ren W, Tian GY, et al. Low energy impact damage detection in CFRP using eddy current pulsed thermography. *Compos Struct* 2016; 143: 352–361.
125. Tenek LH, Henneke EG II and Gunzburger MD. Vibration of delaminated composite plates and some applications to non-destructive testing. *Compos Struct* 1993; 23: 253–262.
126. Rantala J, Wu D and Busse G. Amplitude-modulated lock-in vibrothermography for NDE of polymers and composites. *Res Nondestruct Eval* 1996; 7: 215–228.
127. Pieczonka L, Aymerich F, Brozek G, et al. Modelling and numerical simulations of vibrothermography for impact damage detection in composites structures. *Struct Control Health Monit* 2013; 20: 626–638.
128. Palumbo D, Ancona F and Galietti U. Quantitative damage evaluation of composite materials with microwave thermographic technique: feasibility and new data analysis. *Meccanica* 2015; 50: 443–459.
129. Foudazi A, Edwards CA, Ghasr MT, et al. Active microwave thermography for defect detection of CFRP-strengthened cement-based materials. *IEEE Trans Instrum Meas* 2016; 65: 2612–2620.
130. Wu D and Busse G. Lock-in thermography for nondestructive evaluation of materials. *Rev Génér Therm* 1998; 37: 693–703.
131. Yang R and He Y. Optically and non-optically excited thermography for composites: a review. *Infrared Phys Technol* 2016; 75: 26–50.
132. ASTM E2582:2019. Standard practice for infrared flash thermography of composite panels and repair patches used in aerospace applications.
133. Tonouchi M. Cutting-edge terahertz technology. *Nat Photon* 2007; 1: 97–105.
134. Sirtori C. Bridge for the terahertz gap. *Nature* 2002; 417: 132–133.
135. Auston DH, Cheung KP, Valdmanis JA, et al. Cherenkov radiation from femtosecond optical pulses in electro-optic media. *Phys Rev Lett* 1984; 53: 1555–1558.
136. Fattinger C and Grischkowsky D. Point source terahertz optics. *Appl Phys Lett* 1988; 53: 1480–1482.
137. Dobroiu A, Otani C and Kawase K. Terahertz-wave sources and imaging applications. *Meas Sci Technol* 2006; 17: R161–R174.
138. Guillet JP, Recur B, Frederique L, et al. Review of terahertz tomography techniques. *J Infrared Millim Terahertz Waves* 2014; 35: 382–411.

139. Redo-Sanchez A, Heshmat B, Aghasi A, et al. Terahertz time-gated spectral imaging for content extraction through layered structures. *Nat Commun* 2016; 7: 12665.
140. Wang Q, Zhou H, Liu M, et al. Study of the skin depth and defect detection in carbon fiber composites with terahertz waves. *Optik* 2019; 178: 1035–1044.
141. Dong J, Pomarède P, Chehami L, et al. Visualization of subsurface damage in woven carbon fiber-reinforced composites using polarization-sensitive terahertz imaging. *NDT E Int* 2018; 99: 72–79.
142. Zhang H, Sfarra S, Sarasini F, et al. Thermographic non-destructive evaluation for natural fiber-reinforced composite laminates. *Appl Sci* 2018; 8: 240.
143. Han DH and Kang LH. Nondestructive evaluation of GFRP composite including multi-delamination using THz spectroscopy and imaging. *Compos Struct* 2018; 185: 161–175.
144. Yahng JS, Park CS, Don Lee H, et al. High-speed frequency-domain terahertz coherence tomography. *Opt Express* 2016; 24: 1053–1061.
145. Zhang J, Li W, Cui HL, et al. Nondestructive evaluation of carbon fiber reinforced polymer composites using reflective terahertz imaging. *Sensors* 2016; 16: 875.
146. Lopato P. Double-sided terahertz imaging of multi-layered glass fiber-reinforced polymer. *Appl Sci* 2017; 7: 661.
147. Okano M and Watanabe S. Internal status of visibly opaque black rubbers investigated by terahertz polarization spectroscopy: fundamentals and applications. *Polymers* 2018; 11: 9.
148. Jansen C, Wietzke S, Peters O, et al. Terahertz imaging: applications and perspectives. *Appl Opt* 2010; 49: E48–E57.
149. Leendertz JA. Interferometric displacement measurement on scattering surfaces utilizing speckle effect. *J Phys E* 1970; 3: 214–218.
150. Leendertz JA and Butters JN. An image-shearing speckle-pattern interferometer for measuring bending moments. *J Phys E* 1973; 6: 1107–1110.
151. Chau FS, Toh SL, Tay CJ, et al. Some examples of non-destructive flaw detection by shearography. *J Nondestruct Eval* 1989; 8: 225–234.
152. Toh SL, Shang HM, Chau FS, et al. Flaw detection in composites using time-average shearography. *Opt Laser Technol* 1991; 23: 25–30.
153. De Angelis G, Meo M, Almond DP, et al. A new technique to detect defect size and depth in composite structures using digital shearography and unconstrained optimization. *NDT E Int* 2012; 45: 91–96.
154. Tyson J II and Newman JW. *Apparatus and method for detecting leaks in packages*. US5307139A Patent, 1994.
155. Rubayi NA and Liew SH. Vacuum stressing technique for composite laminates inspection by optical method. *Exp Tech* 1989; 13: 17–20.
156. Pieczonka L, Aymerich F and Staszewski WJ. Impact damage detection in light composite sandwich panels. *Proced Eng* 2014; 88: 216–221.
157. Groves RM, James SW and Tatam RP. Full surface strain measurement using shearography. In: Farrell PV, Chiang FP, Mercer CR, et al. (eds) *Optical diagnostics for fluids, solids, and combustion*. Bellingham, WA: International Society for Optics and Photonics, 2001, pp.142–152.
158. Groves RM, Chehura E, Li W, et al. Surface strain measurement: a comparison of speckle shearing interferometry and optical fibre Bragg gratings with resistance foil strain gauges. *Meas Sci Technol* 2007; 18: 1175–1184.
159. Tay CJ, Toh SL, Shang HM, et al. Direct determination of second-order derivatives in plate bending using multiple-exposure shearography. *Opt Laser Technol* 1994; 26: 91–98.
160. Mohan NK. The influence of multiple-exposure recording on curvature pattern using multi-aperture speckle shear interferometry. *Opt Commun* 2000; 186: 259–263.
161. Wang K, Tieu AK and Li E. Influence of displacement and its first- and second-order derivative components on curvature fringe formations in speckle shearography. *Appl Opt* 2002; 41: 4557–4561.
162. Tay CJ and Fu Y. Determination of curvature and twist by digital shearography and wavelet transforms. *Opt Lett* 2005; 30: 2873–2875.
163. Hung YY. Applications of digital shearography for testing of composite structures. *Compos Part B Eng* 1999; 30: 765–773.
164. Pechersky MJ. Determination of residual stresses by thermal relaxation and speckle correlation interferometry. *Strain* 2002; 38: 141–149.
165. Parlevliet PP, Bersee HEN and Beukers A. Residual stresses in thermoplastic composites – a study of the literature – part II: experimental techniques. *Compos Part A Appl Sci Manuf* 2007; 38: 651–665.
166. Lee JR, Molimard J, Vautrin A, et al. Application of grating shearography and speckle shearography to mechanical analysis of composite material. *Compos Part A Appl Sci Manuf* 2004; 35: 965–976.
167. Lee JR, Yoon DJ, Kim JS, et al. Investigation of shear distance in Michelson interferometer-based shearography for mechanical characterization. *Meas Sci Technol* 2008; 19: 115303.
168. Shang HM, Hung YY, Luo WD, et al. Surface profiling using shearography. *Opt Eng* 2000; 39: 23–31.
169. Sim CW, Chau FS and Toh SL. Vibration analysis and non-destructive testing with real-time shearography. *Opt Laser Technol* 1995; 27: 45–49.
170. Valera JDR and Jones JDC. Vibration analysis by modulated time-averaged speckle shearing interferometry. *Meas Sci Technol* 1995; 6: 965–970.
171. Huang JR, Ford HD and Tatam RP. Heterodyning of speckle shearing interferometers by laser diode wavelength modulation. *Meas Sci Technol* 1996; 7: 1721.
172. Huang YH, Ng SP, Liu L, et al. NDT&E using shearography with impulsive thermal stressing and clustering phase extraction. *Opt Laser Eng* 2009; 47: 774–781.
173. Liu Z, Gao J, Xie H, et al. NDT capability of digital shearography for different materials. *Opt Laser Eng* 2011; 49: 1462–1469.
174. Abou-Khousa MA, Ryley A, Kharkovsky S, et al. Comparison of X-ray, millimeter wave, shearography and through-transmission ultrasonic methods for inspection of honeycomb composites. *AIP Conf Proc* 2007; 894: 999–1006.

175. Nyongesa HO, Otieno AW and Rosin PL. Neural fuzzy analysis of delaminated composites from shearography imaging. *Compos Struct* 2001; 54: 313–318.
176. Hung YY. Shearography and applications in experimental mechanics. *Proc SPIE* 1997; 2921: 1–28.
177. Francis D, Tatam RP and Groves RM. Shearography technology and applications: a review. *Meas Sci Technol* 2010; 21: 102001.
178. Xie X and Zhou Z. Shearographic nondestructive testing for high-pressure composite tubes. *SAE Int* 2018; 1: 1219.
179. Macedo FJ, Benedet ME, Fantin AV, et al. Inspection of defects of composite materials in inner cylindrical surfaces using endoscopic shearography. *Opt Laser Eng* 2018; 104: 100–108.
180. ASTM E2581:2014. Standard practice for shearography of polymer matrix composites and sandwich core materials in aerospace applications.
181. Newman JW. *Method and apparatus for contrast enhanced photography of wind turbine blades*. US20160063350A1 Patent, 2019.
182. Steinchen W, Yang L, Kupfer G, et al. Non-destructive testing of aerospace composite materials using digital shearography. *Proc IMechE, Part G: J Aerospace Engineering* 1998; 212: 21–30.
183. Pezzoni R and Krupka R. Laser-shearography for non-destructive testing of large-area composite helicopter structures. *Insight Wigst Northampton* 2001; 43: 244–248.
184. Yusof MY, Loganathan TM, Burhan I, et al. Shearography technique on inspection of advanced aircraft composite material. *IOP Conf Ser Mater Sci Eng* 2019; 554: 12009.
185. Pagliarulo V, Farroni F, Ferraro P, et al. Combining ESPI with laser scanning for 3D characterization of racing tyres sections. *Opt Laser Eng* 2018; 104: 71–77.
186. Kadlec M and Růžek R. A comparison of laser shearography and C-scan for assessing a glass/epoxy laminate impact damage. *Appl Compos Mater* 2012; 19: 393–407.
187. Ibrahim JS, Petzing JN and Tyrer JR. Deformation analysis of aircraft wheels using a speckle shearing interferometer. *Proc IMechE, Part G: J Aerospace Engineering* 2004; 218: 287–295.
188. Bisle WJ, Scherling D, Kalms MK, et al. Improved shearography for use on optical non cooperating surfaces under daylight conditions. *AIP Conf Proc* 2001; 557: 1928–1935.
189. Vollen MW, Vikhagen E, Wang G, et al. Application of shearography techniques for vibration characterization and damage detection in sandwich structures, 2005, <https://apps.dtic.mil/dtic/tr/fulltext/u2/a471574.pdf>
190. Pickering SG and Almond DP. Comparison of the defect detection capabilities of flash thermography and vibration excitation shearography. *Insight Nondestruct Test Cond Monit* 2010; 52: 78–81.
191. Ochôa P, Infante V, Silva JM, et al. Detection of multiple low-energy impact damage in composite plates using Lamb wave techniques. *Compos Part B Eng* 2015; 80: 291–298.
192. Tyson J II and Newman JW. *Apparatus and method for performing electronic shearography*. US5094528A Patent, 1992.
193. Peters WH and Ranson WF. Digital imaging techniques in experimental stress analysis. *Opt Eng* 1982; 21: 427–431.
194. McCormick N and Lord J. Digital image correlation. *Mater Today* 2010; 13: 52–54.
195. MESOCOS MS & CS. DIC measurement in engineering applications, 2015, pp.1–13, <http://image-correlation.com/assets/files/MESOCOS-DIC.pdf>
196. Dong YL and Pan B. A review of speckle pattern fabrication and assessment for digital image correlation. *Exp Mech* 2017; 57: 1161–1181.
197. Pan B. Digital image correlation for surface deformation measurement: historical developments, recent advances and future goals. *Meas Sci Technol* 2018; 29: 82001.
198. Hild F, Bouterf A and Roux S. Damage measurements via DIC. *Int J Fract* 2015; 191: 77–105.
199. Aparna ML, Chaitanya G, Srinivas K, et al. Fatigue testing of continuous GFRP composites using digital image correlation (DIC) technique: a review. *Mater Today Proc* 2015; 2: 3125–3131.
200. Caminero MA, Lopez-Pedrosa M, Pinna C, et al. Damage assessment of composite structures using digital image correlation. *Appl Compos Mater* 2014; 21: 91–106.
201. Willems A, Lomov SV, Verpoest I, et al. Drape-ability characterization of textile composite reinforcements using digital image correlation. *Opt Laser Eng* 2009; 47: 343–351.
202. Elhajjar RF and Shams SS. A new method for limit point determination in composite materials containing defects using image correlation. *Compos Sci Technol* 2016; 122: 140–148.
203. Catalanotti G, Camanho PP, Xavier J, et al. Measurement of resistance curves in the longitudinal failure of composites using digital image correlation. *Compos Sci Technol* 2010; 70: 1986–1993.
204. Dias GF, de Moura MFSF, Chousal JAG, et al. Cohesive laws of composite bonded joints under mode I loading. *Compos Struct* 2013; 106: 646–652.
205. Furtado C, Arteiro A, Catalanotti G, et al. Selective ply-level hybridisation for improved notched response of composite laminates. *Compos Struct* 2016; 145: 1–14.
206. Smyl D, Antin KN, Liu D, et al. Coupled digital image correlation and quasi-static elasticity imaging of inhomogeneous orthotropic composite structures. *Inverse Probl* 2018; 34: 124005.
207. Sarasini F, Tirillò J, D'Altilia S, et al. Damage tolerance of carbon/flax hybrid composites subjected to low velocity impact. *Compos Part B Eng* 2016; 91: 144–153.
208. Wang Y, Lava P, Coppeters S, et al. Investigation of the uncertainty of DIC under heterogeneous strain states with numerical tests. *Strain* 2012; 48: 453–462.
209. Manzato S, Di Lorenzo E, and Mäkel P. Enhancing standard GVT measurements with digital image correlation. In *Structural Health Monitoring, Photogrammetry & DIC* (Volume 6). Cham: Springer, 2019, pp. 31–41.
210. Liu Y, Nelson J, Holzner C, et al. Recent advances in synchrotron-based hard X-ray phase contrast imaging. *J Phys D Appl Phys* 2013; 46: 494001.
211. Momose A. Recent advances in X-ray phase imaging. *Jpn J Appl Phys* 2005; 44: 6355–6367.

212. Banhart J, Borbély A, Dzieciol K, et al. X-ray and neutron imaging – complementary techniques for materials science and engineering. *Int J Mater Res* 2010; 101: 1069–1079.
213. Fitzpatrick ME and Lodini A. *Analysis of residual stress by diffraction using neutron and synchrotron radiation*. Boca Raton, FL: CRC Press, 2003.
214. Zhou XL and Chen SH. Theoretical foundation of X-ray and neutron reflectometry. *Phys Rep* 1995; 257: 223–348.
215. Allen AJ, Hutchings MT, Windsor CG, et al. Neutron diffraction methods for the study of residual stress fields. *Adv Phys* 1985; 34: 445–473.
216. Hutchings MT, Withers PJ, Holden TM, et al. *Introduction to the characterization of residual stress by neutron diffraction*. Boca Raton, FL: CRC press, 2005.
217. Wang B. *Viscoelastically prestressed composites: towards process optimisation and application to morphing structures*. Hull: University of Hull, 2016.
218. Garcea SC, Wang Y and Withers PJ. X-ray computed tomography of polymer composites. *Compos Sci Technol* 2018; 156: 305–319.
219. Caballero L, Colomer FA, Bellot AC, et al. Gamma-ray imaging system for real-time measurements in nuclear waste characterisation. *J Instrum* 2018; 13: P03016.
220. Garcea SC, Sinclair I, Spearing SM, et al. Mapping fibre failure in situ in carbon fibre reinforced polymers by fast synchrotron X-ray computed tomography. *Compos Sci Technol* 2017; 149: 81–89.
221. Wang B, Tan D, Lee TL, et al. Ultrafast synchrotron X-ray imaging studies of microstructure fragmentation in solidification under ultrasound. *Acta Mater* 2018; 144: 505–515.
222. Tavares PF, Leemann SC, Sjöström M, et al. The MAXIV storage ring project. *J Synchrotron Radiat* 2014; 21: 862–877.
223. Gruner SM. Study for a proposed phase I energy recovery linac (ERL) synchrotron light source at Cornell University, 2001, https://www.classe.cornell.edu/rsrc/Home/Research/ERL/ERLPubs2001/ERLPub01_7.pdf
224. Cool TA, McIlroy A, Qi F, et al. Photoionization mass spectrometer for studies of flame chemistry with a synchrotron light source. *Rev Sci Instrum* 2005; 76: 94102.
225. Bilderback DH, Elleaume P and Weckert E. Review of third and next generation synchrotron light sources. *J Phys B Atom Mol Opt Phys* 2005; 38: S773–S797.
226. Di Cicco A, Aquilanti G, Minicucci M, et al. Novel XAFS capabilities at ELETTRA synchrotron light source. *J Phys Conf Ser* 2009; 190: 12043.
227. Jiang M, Yang X, Xu H, et al. Shanghai synchrotron radiation facility. *Chin Sci Bull* 2009; 54: 4171.
228. Eriksson M, Ahlbäck J, Andersson Å, et al. The MAX IV synchrotron light source. In: *Proceedings of IPAC2011*, San Sebastián, 2011, pp.1–4, <https://lup.lub.lu.se/search/ws/files/6392076/2541320.pdf>
229. Liu L, Milas N, Mukai AHC, et al. The SIRIUS project. *J Synchrotron Radiat* 2014; 21: 904–911.
230. Jiao Y, Xu G, Cui XH, et al. The HEPS project. *J Synchrotron Radiat* 2018; 25: 1611–1618.
231. Zhao Z. Synchrotron light sources. *Synchrotron Radiat Mater Sci* 2018; 1: 1–33.
232. ASTM E2033:2017. Standard practice for radiographic examination using computed radiography (photostimulable luminescence method).
233. ASTM E2662:2015. Standard practice for radiographic examination of flat panel composites and sandwich core materials used in aerospace applications.
234. Chadwick J. Possible existence of a neutron. *Nature* 1932; 129: 312.
235. Baruchel J, Hodeau JL, Lehmann MS, et al. *Neutron and synchrotron radiation for condensed matter studies*. Berlin: Springer, 1993.
236. Santisteban JR, Daymond MR, James JA, et al. ENGIN-X: a third-generation neutron strain scanner. *J Appl Crystallogr* 2006; 39: 812–825.
237. Wang B, Seffen KA, Guest SD, et al. *In-situ* micromechanical shear failure of a bistable composite tape-spring. 2020 (under review).
238. Aksenov VL. Reactor neutron sources. In: Jacob M and Schopper H. (eds) *Large facilities in physics: proceedings of the 5th EPS international conference on large facilities*. Singapore: World Scientific, 1995, pp.273–291.
239. Richter D and Springer T. A twenty years forward look at neutron scattering facilities in the OECD countries and Russia, 1998, http://www-llb.cea.fr/rapport/oecd_esf_1998.pdf
240. Shinohara T, Kai T, Oikawa K, et al. Final design of the energy-resolved neutron imaging system ‘RADEN’ at J-PARC. *J Phys Conf Ser* 2016; 746: 12007.
241. Minniti T, Watanabe K, Burca G, et al. Characterization of the new neutron imaging and materials science facility IMAT. *Nucl Instrum Meth Phys Res Sect A Accel Spectromet Detect Assoc Equip* 2018; 888: 184–195.
242. Vontobel P, Lehmann EH, Hassanein R, et al. Neutron tomography: method and applications. *Phys B Condens Matter* 2006; 385–386: 475–480.
243. Kockelmann W, Zhang SY, Kelleher JF, et al. IMAT – a new imaging and diffraction instrument at ISIS. *Phys Procedia* 2013; 43: 100–110.
244. Kockelmann W, Minniti T, Pooley D, et al. Time-of-flight neutron imaging on IMAT@ISIS: a new user facility for materials science. *J Imaging* 2018; 4: 47.
245. Woracek R, Santisteban J, Fedrigo A, et al. Diffraction in neutron imaging – a review. *Nucl Instrum Meth Phys Res Sect A Accel Spectromet Detect Assoc Equip* 2018; 878: 141–158.
246. Strobl M, Manke I, Kardjilov N, et al. Advances in neutron radiography and tomography. *J Phys D Appl Phys* 2009; 42: 243001.
247. Kardjilov N, Manke I, Woracek R, et al. Advances in neutron imaging. *Mater Today* 2018; 21: 652–672.
248. Vavilov VP and Burleigh DD. Review of pulsed thermal NDT: physical principles, theory and data processing. *NDT E Int* 2015; 73: 28–52.
249. Atsushi M, Wataru Y, Kazuhiro K, et al. X-ray phase imaging: from synchrotron to hospital. *Philos Trans A Math Phys Eng Sci* 2014; 372: 20130023.
250. Pracht M and Swiderski W. Analysis of the possibility of non-destructive testing to detect defects in multi-layered composites reinforced fibers by optical IR thermography. *Compos Struct* 2019; 213: 204–208.

251. Stoik C, Bohn M and Blackshire J. Nondestructive evaluation of aircraft composites using reflective terahertz time domain spectroscopy. *NDT E Int* 2010; 43: 106–115.
252. Ye Y, Ma K, Zhou H, et al. An automated shearography system for cylindrical surface inspection. *Measurement* 2019; 135: 400–405.
253. Senck S, Scheerer M, Revol V, et al. Microcrack characterization in loaded CFRP laminates using quantitative two- and three-dimensional X-ray dark-field imaging. *Compos Part A Appl Sci Manuf* 2018; 115: 206–214.
254. De Simone ME, Cuomo S, Ciampa F, et al. Acoustic emission localization in composites using the signal power method and embedded transducers. In: Gyeke-nyesi AL, Yu TY, Wu HF, et al. (eds) *Nondestructive characterization and monitoring of advanced materials, aerospace, civil infrastructure, and transportation XIII*. Bellingham, WA: International Society for Optics and Photonics, 2019, p.1097110.
255. Ashir M, Nocke A, Bulavinov A, et al. Sampling phased array technology for the detection of voids in carbon fiber-reinforced plastics. *J Text Inst* 2019; 110: 1703–1709.
256. Podymova NB, Kalashnikov IE, Bolotova LK, et al. Laser-ultrasonic nondestructive evaluation of porosity in particulate reinforced metal-matrix composites. *Ultrasonics* 2019; 99: 105959.
257. Bendada A, Sfarra S, Genest M, et al. How to reveal subsurface defects in Kevlar® composite materials after an impact loading using infrared vision and optical NDT techniques? *Eng Fract Mech* 2013; 108: 195–208.
258. Yang F, Ye X, Qiu Z, et al. The effect of loading methods and parameters on defect detection in digital shearography. *Result Phys* 2017; 7: 3744–3755.
259. Centea T and Hubert P. Measuring the impregnation of an out-of-autoclave prepreg by micro-CT. *Compos Sci Technol* 2011; 71: 593–599.
260. Alam MK, Khan MA, Lehmann EH, et al. Study of the water uptake and internal defects of jute-reinforced polymer composites with a digital neutron radiography technique. *J Appl Polym Sci* 2007; 105: 1958–1963.
261. Kam E, Reyhancan IA and Biyik R. A portable fast neutron radiography system for non-destructive analysis of composite materials. *Nukleonika* 2019; 64: 97–101.
262. Saeedifar M, Fotouhi M, Ahmadi Najafabadi M, et al. Prediction of quasi-static delamination onset and growth in laminated composites by acoustic emission. *Compos Part B Eng* 2016; 85: 113–122.
263. Laureti S, Khalid Rizwan M, Malekmohammadi H, et al. Delamination detection in polymeric ablative materials using pulse-compression thermography and air-coupled ultrasound. *Sensors* 2019; 19: 2198.
264. Ryu CH, Park SH, Kim DH, et al. Nondestructive evaluation of hidden multi-delamination in a glass-fiber-reinforced plastic composite using terahertz spectroscopy. *Compos Struct* 2016; 156: 338–347.
265. Pagliarulo V, Papa I, Lopresto V, et al. Impact damage investigation on glass fiber-reinforced plate laminates at room and lower temperatures through ultrasound testing and electronic speckle pattern interferometry. *J Mater Eng Perform* 2019; 28: 3301–3308.
266. Szebényi G and Hliva V. Detection of delamination in polymer composites by digital image correlation – experimental test. *Polymers* 2019; 11: 523.
267. Ellison A and Kim H. Shadowed delamination area estimation in ultrasonic C-scans of impacted composites validated by X-ray CT. *J Compos Mater* 2019; 52: 549–561.
268. Yi Q, Tian GY, Malekmohammadi H, et al. New features for delamination depth evaluation in carbon fiber reinforced plastic materials using eddy current pulse-compression thermography. *NDT E Int* 2019; 102: 264–273.
269. Li H and Zhou Z. Detection and characterization of debonding defects in aeronautical honeycomb sandwich composites using noncontact air-coupled ultrasonic testing technique. *Appl Sci* 2019; 9: 283.
270. Yi Q, Tian GY, Yilmaz B, et al. Evaluation of debonding in CFRP-epoxy adhesive single-lap joints using eddy current pulse-compression thermography. *Compos Part B Eng* 2019; 178: 107461.
271. Dai B, Wang P, Wang TY, et al. Improved terahertz nondestructive detection of debonds locating in layered structures based on wavelet transform. *Compos Struct* 2017; 168: 562–568.
272. Wen Y, Zhang S and Zhang Y. Detection and characterization method for interface bonding defects of new composite materials. *IEEE Access* 2019; 7: 134330–134337.
273. Fernandes H, Zhang H, Ibarra-Castaneda C, et al. Fiber orientation assessment on randomly-oriented strand composites by means of infrared thermography. *Compos Sci Technol* 2015; 121: 25–33.
274. Mendoza A, Schneider J, Parra E, et al. Differentiating 3D textile composites: a novel field of application for digital volume correlation. *Compos Struct* 2019; 208: 735–743.
275. Prade F, Schaff F, Senck S, et al. Nondestructive characterization of fiber orientation in short fiber reinforced polymer composites with X-ray vector radiography. *NDT E Int* 2017; 86: 65–72.
276. Evans LM, Minniti T, Barrett T, et al. Virtual qualification of novel heat exchanger components with the image-based finite element method. In: *Proceedings of the 9th conference on industrial computed tomography (iCT)*, Padova, 2019, https://www.ndt.net/article/ctc2019/papers/iCT2019_Full_paper_24.pdf
277. Dornfeld D. Application of acoustic emission techniques in manufacturing. *NDT E Int* 1992; 25: 259–269.
278. Liu PF, Chu JK, Liu YL, et al. A study on the failure mechanisms of carbon fiber/epoxy composite laminates using acoustic emission. *Mater Des* 2012; 37: 228–235.
279. Lee WJ, Seo BH, Hong SC, et al. Real world application of angular scan pulse-echo ultrasonic propagation imager for damage tolerance evaluation of full-scale composite fuselage. *Struct Health Monit* 2019; 18: 1943–1952.
280. Garcia Perez P, Bouvet C, Chettah A, et al. Effect of unstable crack growth on mode II interlaminar fracture toughness of a thermoplastic PEEK composite. *Eng Fract Mech* 2019; 205: 486–497.
281. Hong S, Liu P, Zhang J, et al. Visual & quantitative identification of cracking in mortar subjected to loads

- using X-ray computed tomography method. *Cem Concr Compos* 2019; 100: 15–24.
282. Zhang P, Wang P, Hou D, et al. Application of neutron radiography in observing and quantifying the time-dependent moisture distributions in multi-cracked cement-based composites. *Cem Concr Compos* 2017; 78: 13–20.
283. Safai M and Wang X. *Synchronized phased array and infrared detector system for moisture detection*. US20190113449A1 Patent, 2019.
284. Federici JF. Review of moisture and liquid detection and mapping using terahertz imaging. *J Infrared Millim Terahertz Waves* 2012; 33: 97–126.
285. De Parscau du Plessix B, Lefébure P, Boyard N, et al. In situ real-time 3D observation of porosity growth during composite part curing by ultra-fast synchrotron X-ray microtomography. *J Compos Mater* 2019; 53: 4105–4116.
286. Alam MK, Khan MA and Lehmann EH. Comparative study of water absorption behavior in biopol[®] and jute-reinforced biopol[®] composite using neutron radiography technique. *J Reinf Plast Compos* 2006; 25: 1179–1187.
287. Oromiehie E, Garbe U and Gangadhara Prusty B. Porosity analysis of carbon fibre-reinforced polymer laminates manufactured using automated fibre placement. *J Compos Mater* 2019; 54: 1217–1231.
288. Wang S, Tran T, Xiang L, et al. Non-destructive evaluation of composite and metallic structures using photo-acoustic method. In: *Proceedings of the AIAA SciTech 2019 forum*, 2019, p.2042, <https://arc.aiaa.org/doi/abs/10.2514/6.2019-2042>
289. Destic F and Bouvet C. Impact damages detection on composite materials by THz imaging. *Case Stud Non-destruct Test Eval* 2016; 6: 53–62.
290. Ranatunga V, Crampton SM and Jegley DC. Impact damage tolerance of composite laminates with through-the-thickness stitches. In: *Proceedings of the AIAA Sci-Tech 2019 forum*, 2019, p.1045, <https://arc.aiaa.org/doi/10.2514/6.2019-1045>
291. Aslan M. Investigation of damage mechanism of flax fibre LPET commingled composites by acoustic emission. *Compos Part B Eng* 2013; 54: 289–297.
292. Siriruk A, Woracek R, Pumplamp SB, et al. Damage evolution in VARTM-based carbon fiber vinyl ester marine composites and sea water effects. *J Sandw Struct Mater* 2019; 21: 2057–2076.
293. Yuan Y and Wang S. Measurement of the energy release rate of compressive failure in composites by combining infrared thermography and digital image correlation. *Compos Part A Appl Sci Manuf* 2019; 122: 59–66.
294. Djabali A, Toubal L, Zitoune R, et al. Fatigue damage evolution in thick composite laminates: combination of X-ray tomography, acoustic emission and digital image correlation. *Compos Sci Technol* 2019; 183: 107815.
295. Lopato P and Chady T. Terahertz examination of fatigue loaded composite materials. *Int J Appl Electromagn Mech* 2014; 45: 613–619.
296. Dia A, Dieng L, Gaillet L, et al. Damage detection of a hybrid composite laminate aluminum/glass under quasi-static and fatigue loadings by acoustic emission technique. *Heliyon* 2019; 5: e01414.
297. Wagner P, Schwarzhaupt O and May M. In-situ X-ray computed tomography of composites subjected to fatigue loading. *Mater Lett* 2019; 236: 128–130.
298. Reid A, Marshall M, Kabra S, et al. Application of neutron imaging to detect and quantify fatigue cracking. *Int J Mech Sci* 2019; 159: 182–194.
299. Aggelis DG, Barkoula NM, Matikas TE, et al. Acoustic structural health monitoring of composite materials: damage identification and evaluation in cross ply laminates using acoustic emission and ultrasonics. *Compos Sci Technol* 2012; 72: 1127–1133.
300. Sfarra S, Regi M, Santulli C, et al. An innovative non-destructive perspective for the prediction of the effect of environmental aging on impacted composite materials. *Int J Eng Sci* 2016; 102: 55–76.
301. Rahani EK, Kundu T, Wu Z, et al. Mechanical damage detection in polymer tiles by THz radiation. *IEEE Sens J* 2011; 11: 1720–1725.
302. Arora H, Hooper PA and Dear JP. Dynamic response of full-scale sandwich composite structures subject to air-blast loading. *Compos Part A Appl Sci Manuf* 2011; 42: 1651–1662.
303. Anisimov AG and Groves RM. EXTREME shearography: high-speed shearography instrument for in-plane surface strain measurements during an impact event. *Proc SPIE* 2019; 11056: 1–8.
304. Sui T, Salvati E, Zhang H, et al. Probing the complex thermo-mechanical properties of a 3D-printed poly(lactide-hydroxyapatite) composite using in situ synchrotron X-ray scattering. *J Adv Res* 2019; 16: 113–122.
305. Stoik CD, Bohn MJ and Blackshire JL. Nondestructive evaluation of aircraft composites using transmissive terahertz time domain spectroscopy. *Opt Express* 2008; 16: 17039–17051.
306. Jiang N, Yu T, Li Y, et al. Hygrothermal aging and structural damage of a jute/poly (lactic acid) (PLA) composite observed by X-ray tomography. *Compos Sci Technol* 2019; 173: 15–23.
307. Chelliah SK, Parameswaran P, Ramasamy S, et al. Optimization of acoustic emission parameters to discriminate failure modes in glass-epoxy composite laminates using pattern recognition. *Struct Health Monit* 2018; 18: 1253–1267.
308. Mahmod MF, Bakar EA, Ramzi R, et al. Artificial neural network application for damages classification in fibreglass pre-impregnated laminated composites (FGLC) from ultrasonic signal. In: Zawawi MAM, Teoh SS, Abdullah NB, et al. (eds) *Proceedings of the 10th international conference on robotics, vision, signal processing and power applications*, Singapore: Springer, 2019, pp.567–573.
309. Saeed N, King N, Said Z, et al. Automatic defects detection in CFRP thermograms, using convolutional neural

- networks and transfer learning. *Infrared Phys Technol* 2019; 102: 103048.
310. Hu C, Duan Y, Liu S, et al. LSTM-RNN-based defect classification in honeycomb structures using infrared thermography. *Infrared Phys Technol* 2019; 102: 103032.
311. Tu W, Zhong S, Shen Y, et al. Neural network-based hybrid signal processing approach for resolving thin marine protective coating by terahertz pulsed imaging. *Ocean Eng* 2019; 173: 58–67.